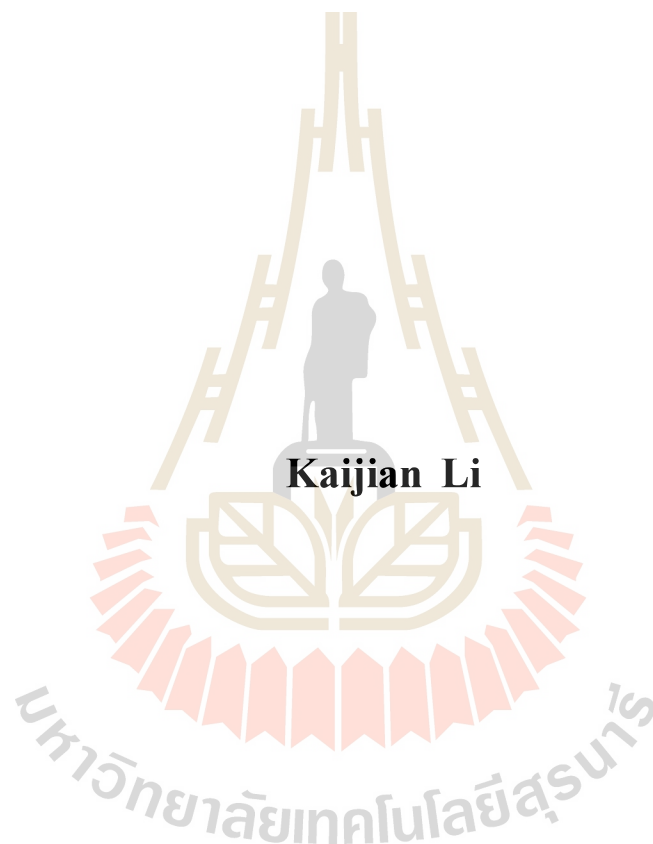


**STUDY OF DOSE RATE IN THE BRAIN MODEL BASED ON
THE NEUTRON BEAM OF SUT-MNSR**



**A Thesis Submitted in Partial Fulfillment of the Requirements for the
Degree of Master of Science in Physics
Suranaree University of Technology
Academic Year 2018**

การศึกษ้อัตราปริมาณรังสีในแบบจำลองสมองจากลำนิวตรอน
ของเครื่องกำเนิดนิวตรอนขนาดเล็ก-มทส.

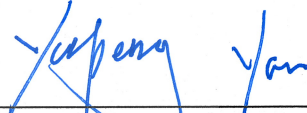


วิทยานิพนธ์นี้เป็นส่วนหนึ่งของการศึกษาตามหลักสูตรปริญญาวิทยาศาสตรมหาบัณฑิต
สาขาวิชาฟิสิกส์
มหาวิทยาลัยเทคโนโลยีสุรนารี
ปีการศึกษา 2561

**STUDY OF DOSE RATE IN THE BRAIN MODEL BASED ON THE
NEUTRON BEAM OF SUT-MNSR**


Suranaree University of Technology has approved thesis submitted in partial fulfillment of the requirements for a Master's Degree.

Thesis Examining Committee




(Prof. Dr. Yupeng Yan)

Chairperson




(Asst. Prof. Dr. Ayut Limphirat)

Member (Thesis Advisor)




(Dr. Nuanwan Sanguansak)

Member



(Asst. Prof. Dr. Khanchai Khosonthongkee)

Member




(Asst. Prof. Dr. Pornrad Srisawad)

Member



(Assoc. Prof. Ft. Lt. Dr. Kontorn Chamniprasart)

Vice Rector for Academic Affairs
and Internationalization



(Assoc. Prof. Dr. Worawat Meevasana)

Dean of Institute of Science

ไคเจียน ลี : การศึกษาอัตราปริมาณรังสีในแบบจำลองสมองจากลำนิวตรอน ของเครื่อง
กำเนิดนิวตรอนขนาดเล็ก-มทส. (STUDY OF DOSE RATE IN THE BRAIN MODEL
BASED ON THE NEUTRON BEAM OF SUT-MNSR) อาจารย์ที่ปรึกษา :
ผู้ช่วยศาสตราจารย์ ดร.อายุทธ ลีมพิรัตน์, 61 หน้า.

รังสีรักษาจากโบรอนจับยัดนิวตรอน (Boron neutron capture therapy : BNCT) เป็นรังสี
รักษาเซลล์มะเร็งแบบจำกดพื้นที่ มีประสิทธิภาพในการรักษาที่ได้รับการยอมรับอย่างดีวิธีการหนึ่ง
สำหรับผู้ป่วยโรคมะเร็งเมื่อเทียบกับรังสีรักษาแบบเดิม ในศตวรรษที่ผ่านมานักวิทยาศาสตร์ชาว
ญี่ปุ่นได้ทดลองใช้เทคนิครังสีรักษาจากโบรอนจับยัดนิวตรอนกับผู้ป่วยโรคมะเร็งศีรษะและคอ
เป็นครั้งแรกของโลก นับตั้งแต่นั้นมาการทดลองและวิจัยทางด้านรังสีรักษาจากโบรอนจับยัด
นิวตรอนเป็นสิ่งที่น่าสนใจและมีการใช้ลำนิวตรอนจากเครื่องปฏิกรณ์นิวเคลียร์สำหรับเทคนิครังสี
รักษาจากโบรอนจับยัดนิวตรอน เครื่องกำเนิดนิวตรอนขนาดเล็ก-มทส. (Miniature Neutron
Source Reactor : SUT-MNSR) อยู่ในระหว่างการออกแบบและสร้างเพื่อใช้สำหรับทดลองและ
วิจัยทางด้านรังสีรักษาจากโบรอนจับยัดนิวตรอน โดยเครื่องกำเนิดนิวตรอนนี้จะให้กำเนิดเทอร์มัล
นิวตรอนหรือนิวตรอนพลังงานต่ำจำนวน 4 ลำและอีพิเทอร์มัลนิวตรอนหรือนิวตรอนพลังงาน
ปานกลางจำนวน 1 ลำ

ก่อนที่เครื่องกำเนิดนิวตรอนขนาดเล็ก-มทส. จะถูกนำมาใช้ในการรักษา อัตราปริมาณรังสีที่
แพร่กระจายเข้าสู่ร่างกายมีความจำเป็นอย่างยิ่งที่ต้องมีการศึกษาและวิจัย ในวิทยานิพนธ์นี้จึงได้
สร้างแบบจำลองสมองแล้วศึกษาการแพร่กระจายและการสะสมของพลังงานของนิวตรอนและ
แกมมาในสมอง โดยวิธีมอนติคาร์โลของการนำพา N อนุภาค ทั้งนี้ได้สร้างแบบจำลองสมอง 2
แบบ ได้แก่แบบสมองปกติและแบบสมองที่มีโบรอนสะสมอยู่โดยโบรอนจำนวน 40 ppm อยู่ที่
บริเวณมะเร็งและโบรอนจำนวน 10 ppm อยู่ที่เนื้อเยื่อสมองปกติ

สาขาวิชาฟิสิกส์
ปีการศึกษา 2561

ลายมือชื่อนักศึกษา KaiJian Li
ลายมือชื่ออาจารย์ที่ปรึกษา [Signature]
ลายมือชื่ออาจารย์ที่ปรึกษาร่วม N. Sangmanee

KAIJIAN LI : STUDY OF DOSE RATE IN THE BRAIN MODEL BASED
ON THE NEUTRON BEAM OF SUT-MNSR. THESIS ADVISOR :
ASST. PROF. AYUT LIMPHIRAT, Ph.D. 61 PP.

BNCT/SUT-MNSR/DOSE RATE DISTRIBUTION/SNYDER BRAIN MODEL

Boron neutron capture therapy (BNCT) is tumor-cell targeted radiotherapy that has a significant superiority over conventional radiotherapies. Since the first treatment of a patient with head and neck cancer in last century in Japan, a number of BNCT facilities have been built using neutron beams from nuclear reactors. The SUT-MNSR (Miniature Neutron Source Reactor) is being built to have four thermal neutron beams and one epithermal neutron beam. The SUT-MNSR epithermal neutron beam is specially designed for BNCT treatments.

In this work we build the brain models and investigate the neutron and gamma dose distributions and the energy deposition in the brain, based on the SUT-MNSR, by applying the Monte Carlo N-Particle Transport Code (MCNP). Two brain models are established according to the different composition of brain tissue, skull and skin, that is, the normal brain model named "Brain Model" and "B-containing Brain Model" where the brain has 40 ppm boron at the tumor area and 10 ppm boron at the normal tissue area.

School of Physics

Academic Year 2018

Student's Signature KaiJian Li

Advisor's Signature [Signature]

Co-advisor's Signature N. Sangvanrak

ACKNOWLEDGEMENT

This thesis is not just a summary of my own work. It could not be accomplished without support from many people. There are many people, to whom I would like to express my sincere words of acknowledgments:

First of all, I would like to thank Asst. Prof. Dr. Ayut Limphirat and Dr. Nuanwan Sanguansak, my thesis advisors, thank you for starting SUT-MNSR project. Thanks for your continual support, discussions and for sharing your knowledge.

I would also like to thank Prof. Dr. Yupeng Yan for introducing me to the particle physics and quantum field theory. In addition to scientific knowledge, I also learned to enjoy daily life from you. I feel very lucky to be your student.

I am also very thankful Asst. Prof. Dr. Khanchai Khosonthongkee, Asst. Prof. Dr. Pornrad Srisawad for comments and suggestions and for accepting to be a member of the examination committee for my thesis.

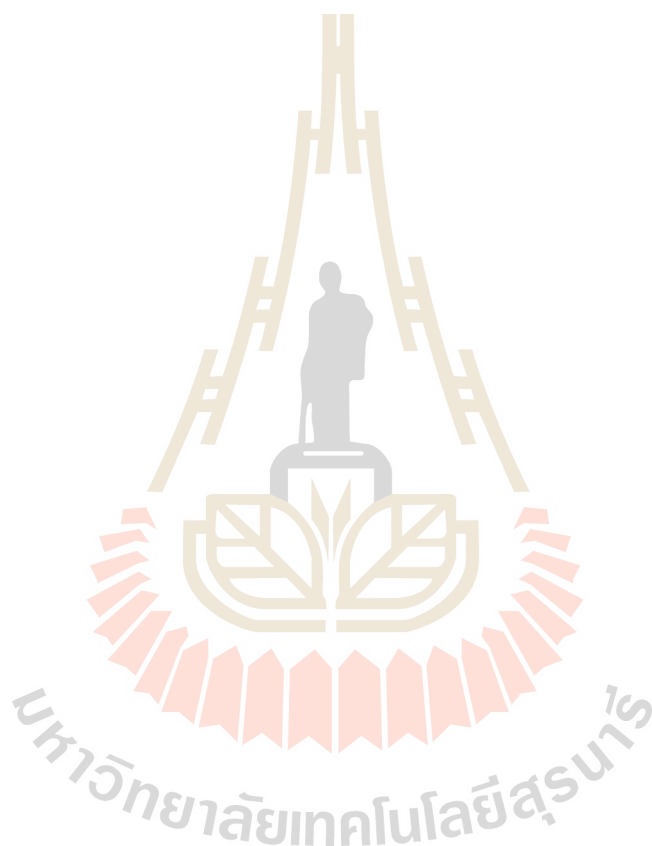
I would like to express my sincere thanks to the staffs at China Institute of Atomic Energy, Prof. Dr. Yiguo Li, Mr. Dan Peng and Mr. Fanjie Cheng for their help during the MCNP simulation method set up.

I am grateful to all of the staffs at SUT BNCT for the holding the workshop about BNCT research and excellent collaborations with China Institute of Atomic Energy.

Special thanks all staffs and students in the School of Physics at SUT for their great support during my study, for all the great times we had together.

Last but not least, my great thanks to my parents: my father, Yiguo Li; my mother Ying Guo. I feel so proud to be your son. Also great thanks to my sisters WenTing Wang and Cuijie Pan for helping in life. You are my inspiration.

Kaijian Li



CONTENTS

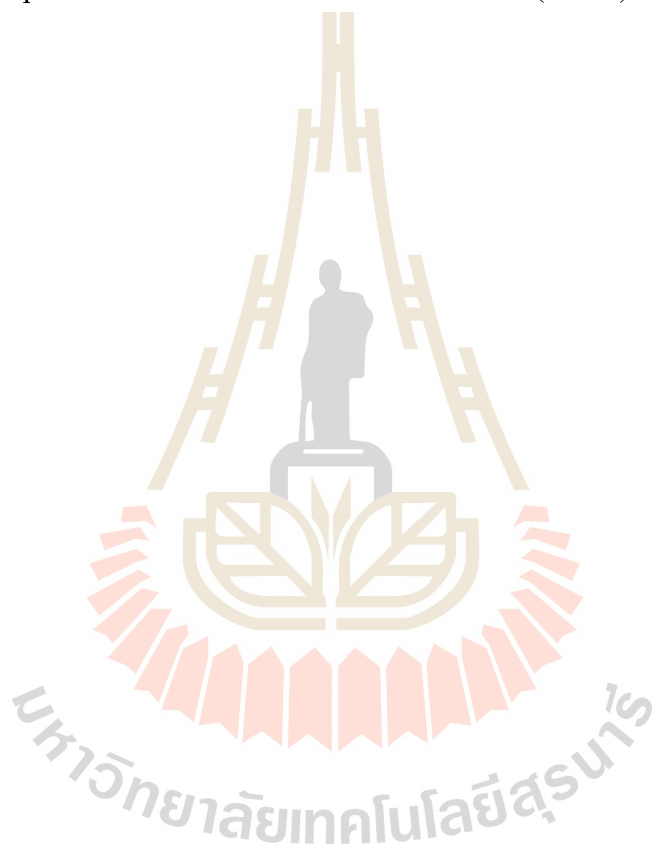
	Page
ABSTRACT IN THAI.....	I
ABSTRACT IN ENGLISH.....	II
ACKNOWLEDGEMENT.....	III
CONTENTS.....	V
LIST OF TABLES.....	VII
LIST OF FIGURES.....	VIII
LIST OF ABBREVIATIONS.....	XI
CHAPTER	
I INTRODUCTION.....	1
1.1 Introduction	1
1.1.1 Boron Neutron Capture Therapy(BNCT).....	1
1.1.2 A General Monte Carlo N-Particle Transport, Version 5.....	3
1.2 Purpose of the study.....	3
II THEORETICAL BACKGROUND.....	5
2.1 Fission Reactor-Based Irradiation Facilities for Neutron Capture Therapy.....	5
2.1.1 Basic principle.....	5
2.1.2 Neutron Moderator and Reflector in Reactor.....	7
2.1.3 The Presence of Gamma Ray for BNCT.....	9

CONTENTS (Continued)

	Page
2.2 Boron Delivery Agent in BNCT Trial.....	10
2.2.1 Requirement of Boron Delivery Agent.....	10
2.2.2 BPA and BSH	10
2.3 BNCT Treatment Planning Based on Monte Carlo Method.....	12
III THE SIMULATION METHOD.....	14
3.1 MCNP Input Document for Reactor Structure.....	14
3.1.1 SUT-MNSR Reactor fuel.....	14
3.1.2 Fuel Assembly.....	15
3.1.3 Whole Input Document.....	16
3.2 MCNP Input Document for Brain Model.....	19
3.3 Tally Method for Brain Model.....	21
3.3.1 Gamma Dose Rate Tally Card.....	23
3.3.2 Neutron Dose Rate Tally Card.....	24
3.3.3 Energy Deposition Tally Card.....	24
IV RESULT AND DISSCUSSION.....	26
4.1 Gamma Dose Rate.....	28
4.2 Neutron Dose Rate.....	30
4.3 Energy Deposition	33
4.4 Discussion and Conclusion.....	36
REFERENCE	39
APPENDIX	43
CURRICULUM VITAE.....	61

LIST OF TALBLES

Table		Page
2.1	Reactors used for BNCT in Japan (Yoshinobu et al., 2006).....	7
3.1	Grid position holes for SUT-MNSR element (CIAE).....	16



LIST OF FIGURES

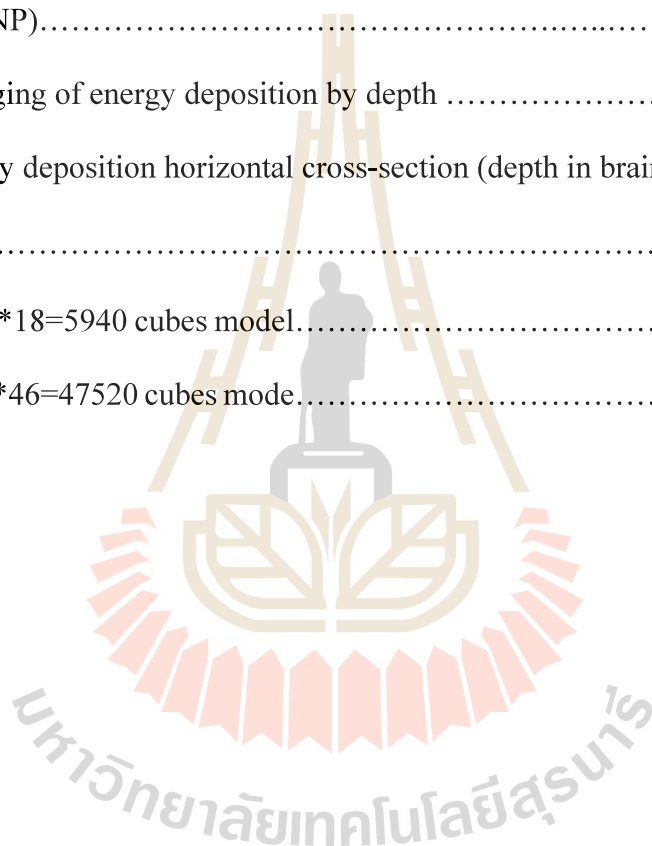
Figure	Page
1.1 Principle of Boron Neutron Capture Therapy (Wikipedia).....	3
2.1 Reactor and number of patients treated by BNCT in Japan (1968-2006) (Yoshinobu et al., 2006).....	6
2.2 Power Distribution where control rod is on Top (CIAE).....	9
2.3 BSH concentration in vascular and other normal tissue (Tsuruta et al., 2008).....	11
2.4 BPA concentration in vascular and other normal tissue (Tsuruta et al., 2008).....	11
2.5 Monte Carlo computational phantom, using a 10mm*10mm*10mm calculation (Zamenhof, 1991).....	12
2.6 Process of treatment planning using JCDS (Kumada et al., 2007).....	13
3.1 Structure Diagram of SUT-MNSR Fuel Element (CIAE).....	14
3.2 Fuel Assembly Diagram (MCNP).....	15
3.3 SUT-MNSR vertical neutron beam for BNCT (CIAE).....	16
3.4 Changes of thermal neutron flux compared with epithermal neutron flux in phantom (Barth et al., 2005).....	17
3.5 SUT-MNSR structure from MNCP (XZ basis).....	18
3.6 SUT-MNSR structure from MNCP (XY basis).....	18
3.7 Cross section of Snyder model (Li et al., 2011).....	19

LIST OF FIGURES (Continued)

Figure	Page
3.8	Material densities and compositions in mass percent (Li et al., 2011).....20
3.9	Snyder brain model from MCNP.....20
3.10	Reactor structure and Snyder brain model all in one from MCNP.....21
3.11	FMESH Mesh model (Kumada et al., 2011).....22
3.12	Photon Flux-to-Dose Rate Conversion Factors (Grande and O’Riordan, 1971).....23
3.13	Neutron Flux-to-Dose Rate Conversion Factors.....24
4.1	Changing of neutron energy spectrum by thickness of water (MCNP).....27
4.2	Gamma dose rate YZ basis (MCNP).....28
4.3	Gamma dose rate XZ basis (MCNP).....29
4.4	Changing of gamma dose rate by depth of brain model (MCNP).....29
4.5	Changing of gamma dose rate by depth of brain model.....30
4.6	Neutron dose rate for brain model YZ basis (MCNP).....31
4.7	Neutron dose rate for B-containing brain model YZ basis (MCNP).....31
4.8	Changing of neutron dose rate for B-containing brain model by depth (MCNP).....32
4.9	Changing of neutron dose rate for brain model by depth (MCNP).....32
4.10	Changing of neutron dose rate for brain model by depth.....33
4.11	Energy deposition for brain model (MCNP).....34
4.12	Energy deposition for B-containing brain model (MCNP).....34

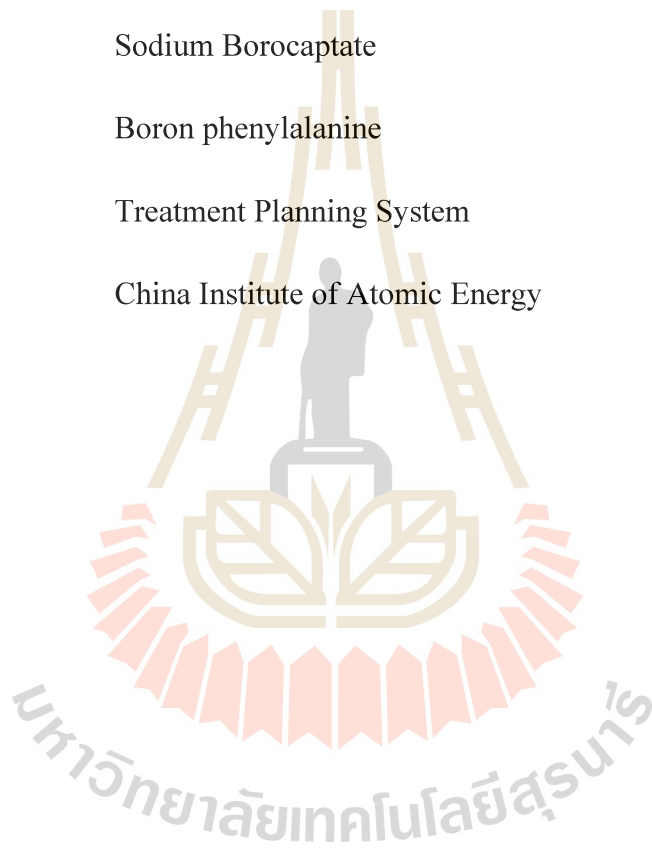
LIST OF FIGURES (Continued)

Figure		Page
4.13	Changing of energy deposition for B-containing brain model by depth (MCNP).....	35
4.14	Changing of energy deposition by depth	35
4.15	Energy deposition horizontal cross-section (depth in brain model 2 cm).....	36
4.16	15*22*18=5940 cubes model.....	37
4.17	30*44*46=47520 cubes mode.....	38



LIST OF ABBREVIATIONS

BNCT	Boron Neutron Capture Therapy
CT	Computed Tomography
BSH	Sodium Borocaptate
BPA	Boron phenylalanine
TPS	Treatment Planning System
CIAE	China Institute of Atomic Energy



CHAPTER I

INTRODUCTION

1.1 Introduction

Cancer is one of the main causes of human death, in 2015, 8.8 million died of cancer worldwide, and the rate of new cases is sharply increasing now. The number of the new cases of head and neck cancer is 390,000 (0.39 million) every year. The estimated total annual economic cost of cancer is 1.16 trillion\$ US.

Radiotherapy and chemotherapy are commonly used in the treatment of cancer, but it is not ideal for the treatment of malignant. Boron neutron capture therapy (BNCT) is an ideal treatment for malignant tumors.

1.1.1 Boron Neutron Capture Therapy (BNCT)

Boron neutron capture therapy (BNCT) is a binary form of radiation therapy using the high propensity of the nonradioactive nuclide boron-10 (^{10}B) to capture thermal neutrons resulting in the prompt nuclear reaction $^{10}\text{B} (n,\alpha) ^7\text{Li}$. The products of this reaction have high linear energy transfer characteristics (α particle approximately $150 \text{ keV}/\mu\text{m}$, ^7Li -nucleus approximately $175 \text{ keV}/\mu\text{m}$). The path lengths of these particles in water or tissues are in the range of $4.5\text{--}10 \mu\text{m}$: hence resulting an energy deposition limited to the diameter of a single cell. Theoretically, therefore, it is possible to selectively irradiate those tumor cells that have taken up a sufficient amount of ^{10}B and simultaneously spare normal cell.

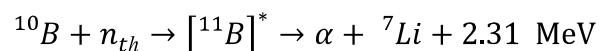
In 1935, Goldhaber discovered very high thermal neutron ($E < 1\text{eV}$) capture cross-section of the ^{10}B (Taylor et al., 1935), and Gordon Locher proposed the therapy of BNCT in 1936 (Locher et al., 1936). After that, a lot of groups in many countries started working on BNCT. The boron containing drugs used for BNCT are BSH (Sweet et al., 1951) and BPA (Conn et al., 2011) (BSH: Boron-Sodium compound and BPA: Boron-Oxygen compound).

First BNCT trial was failed in 1961 in US (Archambeau et al., 1970) due to the use of thermal neutrons, no surgery, low penetration, and the lack of prostate cancer drugs.

During 1968-1978, Dr. H. Hatanaka, an Imperial University of Japan, made a breakthrough by the improvement of BNCT used by thermal neutron, the 5 year survival rate of the treatment of superficial glioma reached an all-time record of 33.3% (Hatanaka et al., 1969).

So far, some clinical trials used by BNCT have been finished by reactor neutron source. The BSH and BPA as the drugs containing boron are commonly used for BNCT, the drugs with the boron enter the cancer cell through the blood circulation, the reaction $^{10}\text{B} (n, \alpha) ^7\text{Li}$ will be happened in cancer cell when a Boron atom in the cancer cell absorbs a thermal neutron.

The basic nuclear reaction is shown in more detail below:



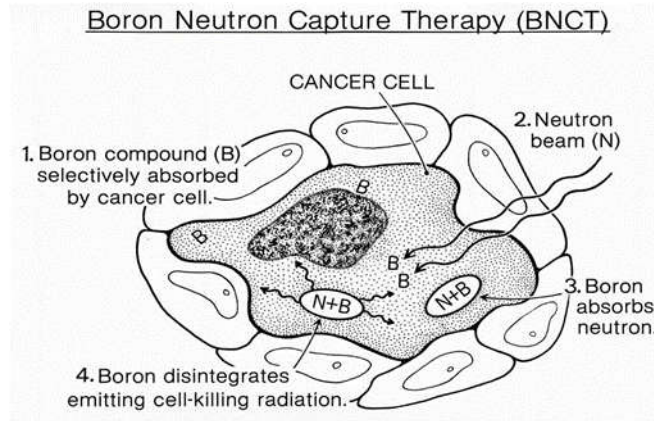


Figure 1.1 Principle of Boron Neutron Capture Therapy (Wikipedia).

1.1.2 A General Monte Carlo N-Particle Transport, Version 5

MCNP is a general-purpose Monte Carlo N-Particle code that can be used for neutron, photon, electron, or coupled neutron/photon/electron transport, including the capability to calculate eigenvalues for critical systems. Point wise cross-section data are used. For neutrons, all reactions are given in a particular cross-section evaluation (such as ENDF/B-VI) are accounted for (X-5 Monte Carlo Team, 2003).

1.2 Purpose of the study

The purpose of this thesis is to investigate the dose rate distribution in brain model based on SUT-MNSR. Now, SUT-MNSR is being designed and built, it will be a new Reactor Facility for BNCT research. According to SUT-MNSR physics design, the parameters of thermal (epithermal) neutron beam show that thermal neutron flux rate is $1.50 \times 10^9 \text{ n} \cdot \text{cm}^{-2} \cdot \text{s}^{-1}$ and epithermal flux rate is $5.4 \times 10^8 \text{ n} \cdot \text{cm}^{-2} \cdot \text{s}^{-1}$, other contamination of fast neutron dose rate and γ dose rate at the exits also meets the IAEA (Barth et al., 2005) standard of BNCT, it is good enough for BNCT. It is important aspect to study

the distributions of dose rate and thermal and epithermal neutron flux in tumor before the BNCT trial.



CHAPTER II

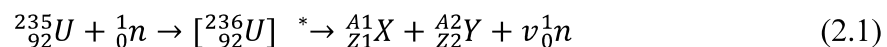
THEORETICAL BACKGROUND

This chapter describes basic knowledge such as reactor fission reaction, reactor neutron moderation, gamma contamination. Moreover, the basic knowledge about BNCT clinical trial is mentioned.

2.1 Fission Reactor-Based Irradiation Facilities for Neutron Capture Therapy

2.1.1 Basic principle

All of kinds of neutron sources for BNCT should provide the suitable neutron beams and the contaminations of fast neutron dose rate. The γ dose rate should meet the IAEA TECDOC 1223 requirement. The thermal or epithermal neutron flux used for patient treatment will enter the tissue and tumor, and the neutron flux will be reduced before it reaches the tumor, it is better if the flux is higher at tumor. Fission reactor-based irradiation facility is one of neutron sources for BNCT clinical trial. Fission reaction is given by



where U is uranium, n is neutron, X and Y are fission products and ν is number of average neutrons product for each time.

The design of SUT-MNSR based on MNSR in China Institute of Atomic Energy is mainly used for BNCT research. Generally, the operating power is 30kW but for BNCT, the power is 45kW.

After the first BNCT clinical trial at Brookhaven, USA, scientists in some countries developed more and more new facilities for BNCT for increasing the thermal neutron flux and decreasing the gamma or other contamination. Typically, KUR, JRR-4 and MIT reactors has been used for BNCT in Japan since 1968. The important parameter for each reactor is shown in Table 2.1. By contrast with SUT-MNSR, SUT-MNST power (30-45kW) much lower than these reactors. So, the gamma contamination (part from reactor core) should be lower also. The cost for operating the reactor will be cheaper.

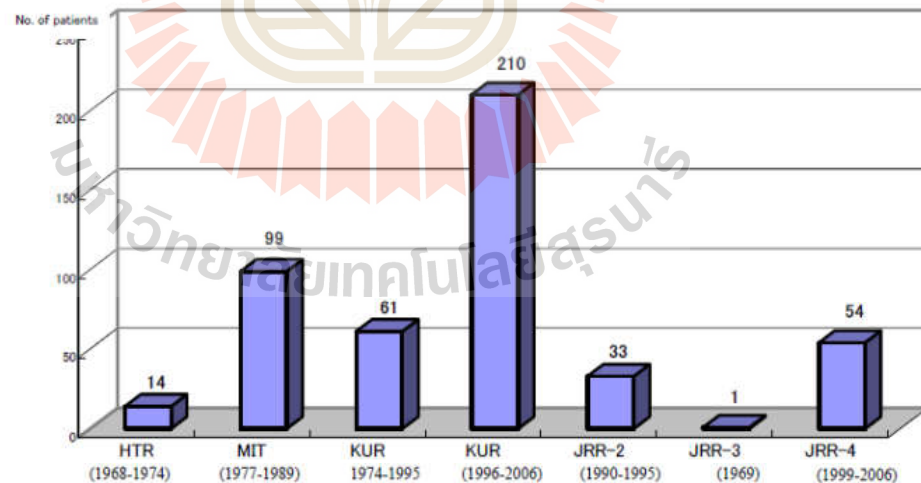


Figure 2.1 Reactor and number of patients treated by BNCT in Japan (1968-2006) (Yoshinobu et al., 2006).

Table 2.1 Reactors used for BNCT in Japan (Yoshinobu et al., 2006).

Reactor	Years used	Power	Flux at medical port
HTR	1968-1974	100KW	3×10^9
JRR-3	1969	10MW	4.8×10^8
MITR	1977-1995	100KW	1.5×10^9
KUR	1974-1995 1996-2006	5MW	3×10^9
		Thermal mode	1.1×10^9
		Epithermal mode	5.1×10^8
IRR	1990-1996	10MW	1.1×10^9
JRR-4	1999-2006	3.5MW	
		Thermal mode	1.9×10^9
		Epithermal mode	2.6×10^9
		Mix mode	2.9×10^9

2.1.2 Neutron Moderator and Reflector in Reactor

Fission neutrons in reactor core have high energy (average $\approx 2\text{MeV}$) (Glasstone et al., 1958), but the neutron beams for BNCT are thermal neutron beam and epithermal neutron beam (low energy $0.1\text{eV} \sim 10\text{keV}$). So the suited moderator and reflector for reactor should be written in physical design for SUT-MNSR. When moderator scattering with neutron:

$$E' = \frac{1}{2} [(1 + \alpha) + (1 - \alpha)\cos\theta_c] E \quad (2.2)$$

$$\alpha = \left(\frac{A-1}{A+1}\right)^2 \quad (2.3)$$

where E' is neutron energy after scattering with moderator nucleus, A = mass number of moderator nucleus, θ_c is scattering angle and E is neutron energy before scattering with moderator nucleus.

When $\theta_c = 0^\circ$: $E' \rightarrow E'_{max} = E$; $\theta_c = 180^\circ$: $E' \rightarrow E'_{min}$. After neutron scattering with moderator nucleus, $E' \in [\alpha E, E]$. If $A=1$, $\alpha=0$, $E'_{min} = 0$ (neutron is possible to loss all of energy). Therefore $H_2 O$ is a suited moderator for reactor to slow down neutron energy. For SUT-MNSR, we shift the spectrum by changing the thickness of water before the SUT-MNSR BNCT outlet. More detailed information will be discussed in next chapter and neutron scattering based on this theory will be simulated by MCNP.

The reflector also can increase the thermal or epithermal neutron beam flux by avoiding the neutron leakage from reactor core. SUT-MNSR reactor reflector made by beryllium. The beryllium reflector includes two parts: beryllium bottom and beryllium side. The bottom beryllium is removed to increase the neutron leakage probability in beam direction and improve the neutron flux density of beam. On the other hand, beryllium reflector can change the power distribution in reactor core to be linear as shown in Figure 2.2.

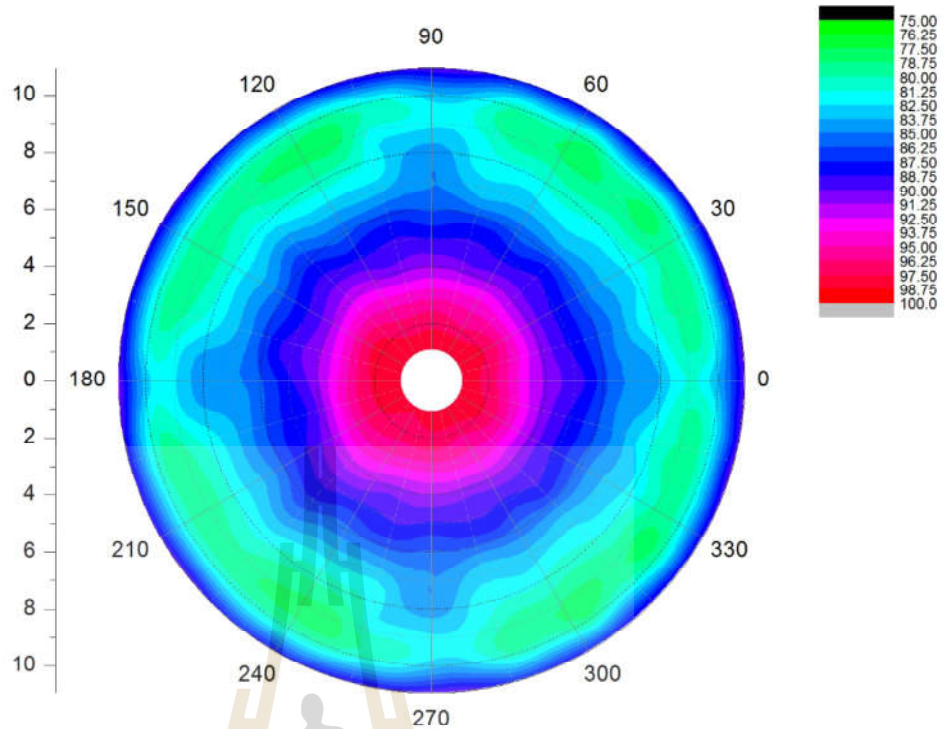


Figure 2.2 Power distribution where control rod is on top (CIAE).

2.1.3 The Presence of Gamma Ray for BNCT

Normally neutrons from a reactor are contaminated by the γ ray. So the gamma is an unavoidable background dose both in normal and tumor tissue, it must be shielded. The presence of photon for BNCT comes from three processes:

1. Prompt γ : fission reaction in the reactor core produces the so called prompt γ .
2. Decay γ : decay of the fission products so called decay γ .
3. Radiative: capture taking place in some of the materials of the reactor and brain.

In this kind of reaction, γ is emitted after a neutron absorption.

The decay γ rate can-not be obtained by MCNP program, so the total calculating result is less than the actual result, but the result of decay γ rate is equal approximately to the value of prompt γ rate. Total results can be obtained by two time of the value of prompt γ rate as shown in the following formula:

$$D \gamma = D \text{ prompt } \gamma + D \text{ decay } \gamma + D (n \gamma) \quad (2.4)$$

$$D \text{ prompt } \gamma \approx D \text{ decay } \gamma \quad (2.5)$$

where D is gamma dose.

2.2 Boron Delivery Agent in BNCT Trial

2.2.1 Requirement of Boron Delivery Agent

In the current research, the B-10 concentration in blood will decrease 60% for boron compound BPA and BSH when the BNCT treatment is started. This change of delivery agent is more and more effective. For an available delivery agent, first, the ratio of boron: $\frac{\text{Brain}+\text{Tumor}}{\text{Blood}} > \frac{4}{1}$; second, tumor region is $\geq 20\mu\text{g/g}$, third, boron can be cleaned as fast as possible at normal tissues and kept long time in tumor. It is important to improve the quality of delivery agent because a good delivery agent can decrease the irradiation time at the same neutron flux rate level. Recent study shows that it is a good method for BNCT treatment when BPA and BSH are injected together to blood and the other one is continuous BPA injection (Barth et al., 2005).

2.2.2 BPA and BSH

Since BNCT have been utilized for brain tumor, there are many reports on the distribution of boron compound (BPA: boron phenylalanine and BSH: sodium borocapate) on normal brain tissues, normal skin and tumor. In this

thesis, for boron dose rate simulation, we set up 40 ppm boron on tumor area and 10 ppm boron on normal tissues. This boron concentration rate is not an accurate result, for clinical treatment, the patient boron concentration rate is measured from blood before the BNCT treatment. Figure 2.3 and Figure 2.4 show BSH and BPA concentration in vascular and other normal tissue.

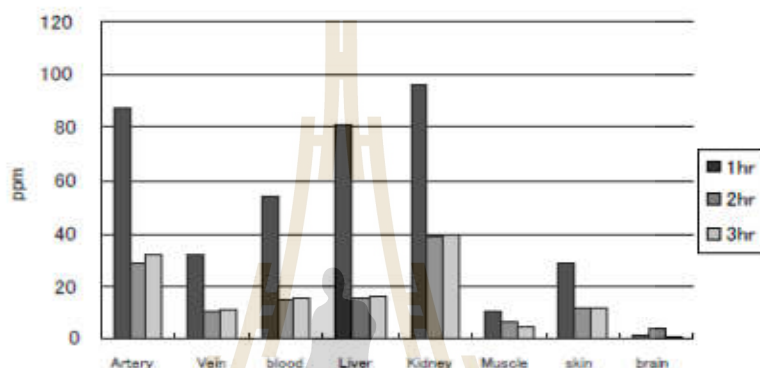


Figure 2.3 BSH concentration in vascular and other normal tissue (Tsuruta et al., 2008).

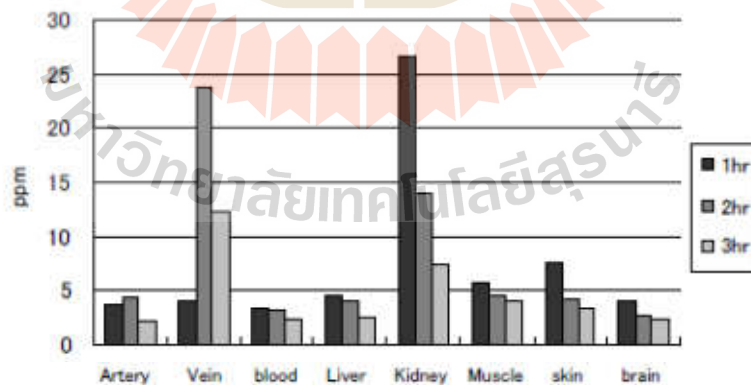


Figure 2.4 BPA concentration in vascular and other normal tissue (Tsuruta et al., 2008).

2.3 BNCT Treatment Planning Based on Monte Carlo Method

BNCT clinical trials need treatment planning to confirm the dosimetry in patient's body. One of available treatment planning systems is Monte Carlo based treatment planning. There are two approach models can be used to calculate dose based on Monte Carlo treatment planning. One approach models is from patient's high spatial resolution (CT etc.) (Nigg et al., 1997). The second approach models is typically with a mesh size of 5-10 mm resolution (Figure 2.5) and calculates the gamma and neutron dose rate in each mesh. Each models has its own advantages. With the changing of computer efficiency to more and more powerful, the first approach model should be selected for BNCT treatment planning. The general purpose Monte Carlo code MCNP (Briesmeister, 1997) not be used for treatment planning. Because MCNP is written for a wide range of diverse radiation transport applications. But it can be used for dose calculation. To make a complete treatment planning system for brain cancer based on SUT-MNSR neutron beam, we start from second model (mesh brain model) to work in this thesis. For more information about brain model and MCNP simulation method, the detail will be written in next chapter.

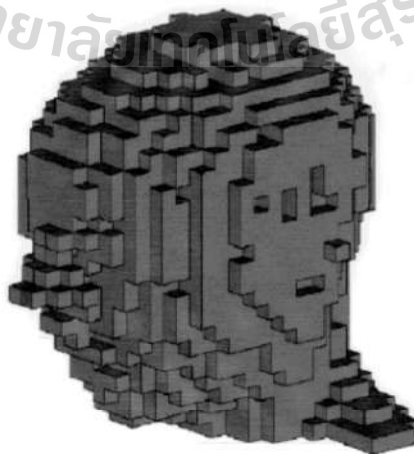


Figure 2.5 Monte Carlo computational phantom using a 10mm*10mm*10mm calculation (Zamenhof et al., 1991).

MCNP calculation should be compared with against the reactor experimental dosimetry result. The result should be including thermal neutron flux, Epi-thermal neutron flux and gamma dose. So it's necessary to set up the experiment to measure the neutron beam and gamma dose after SUT-BNCT building.

There are several MCNP codes currently used for clinical BNCT treatment planning. These are the Idaho National Energy and Engineering Laboratory's SERA (NIGG, et al., 1997), Harvard-MIT's MacNCTPLAN (Zamenhof et al., 1991) and computational dosimetry system for BNCT JCDS (Kumada et al., 2007). JCDS employs a mesh (min: 1*1*1mm) calculation method to simulate the dose rate distribution for patient. This method get the patient's brain model MCNP input document from brain CT data. They put patient's brain voxel model at outlet of neutron beam to calculate the dose rate distribution in three dimensions.

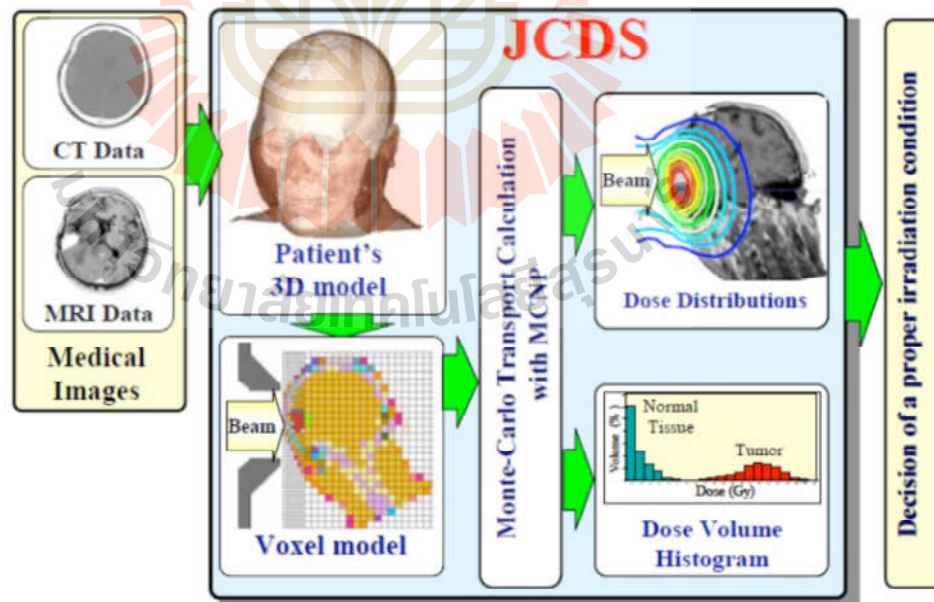


Figure 2.6 Process of treatment planning using JCDS (Kumada et al., 2007).

CHAPTER III

THE SIMULATION METHOD

3.1 MCNP Input Document for Reactor Structure

3.1.1 SUT-MNSR Reactor fuel

The dimensions of reactor core and fuel element in SUT-MNSR are same to those in commercial MNSR, but fuel element pellet is changed from highly enriched uranium U-Al alloy to slightly enriched uranium UO_2 ceramic.

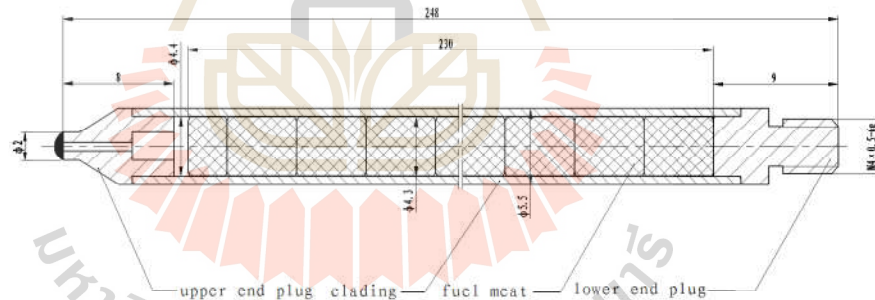


Figure 3.1 Structure Diagram of SUT-MNSR Fuel Element (CIAE).

In fuel element, the core is made of UO_2 with a ^{235}U enrichment of 19.75%, and it has a diameter of 4.3 mm, a length of 230 mm and a density of 10.6 g/cm^3 ; the cladding, made of Zr-4 alloy, has an outside diameter of 5.5 mm, a diameter of 4.4 mm and a density of 6.5 g/cm^3 . Helium gas is filled between fuel cores and cladding; helium gas (1mm) is filled between upper

end plug and core. The upper and lower ends of the element, made of Zr-4 alloy, are 9 mm and 8 mm in length, respectively; the total length of the element is 248 mm. the core of control rod follower is natural uranium UO_2 ceramic, and the material and dimensions of the follower are some to these of fuel element. The height of reactor core active zone is 240 mm.

3.1.2 Fuel Assembly

The reactor core assembly is a “birdcage” structure consisted of upper/lower grids, central control rod conduit and 4 tension rods, which are made of Zr-4 alloy material. The holes for 345 fuel elements are opened on upper and lower grids, and they are uniformly distributed in ten circles, and the “birdcage” and the elements form an integrated reactor core assembly.

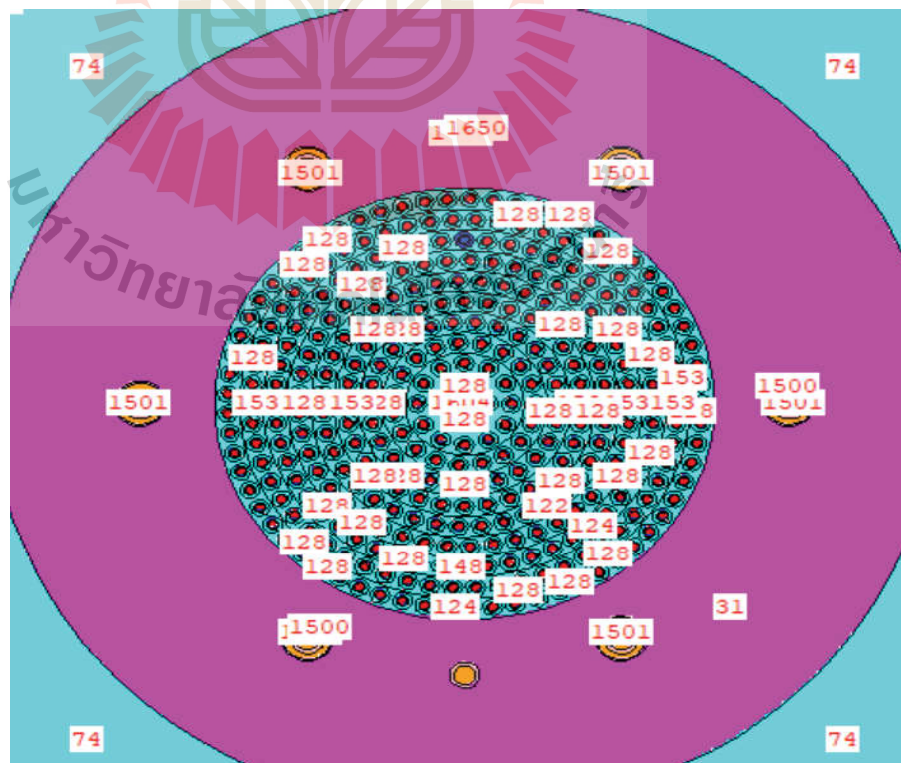


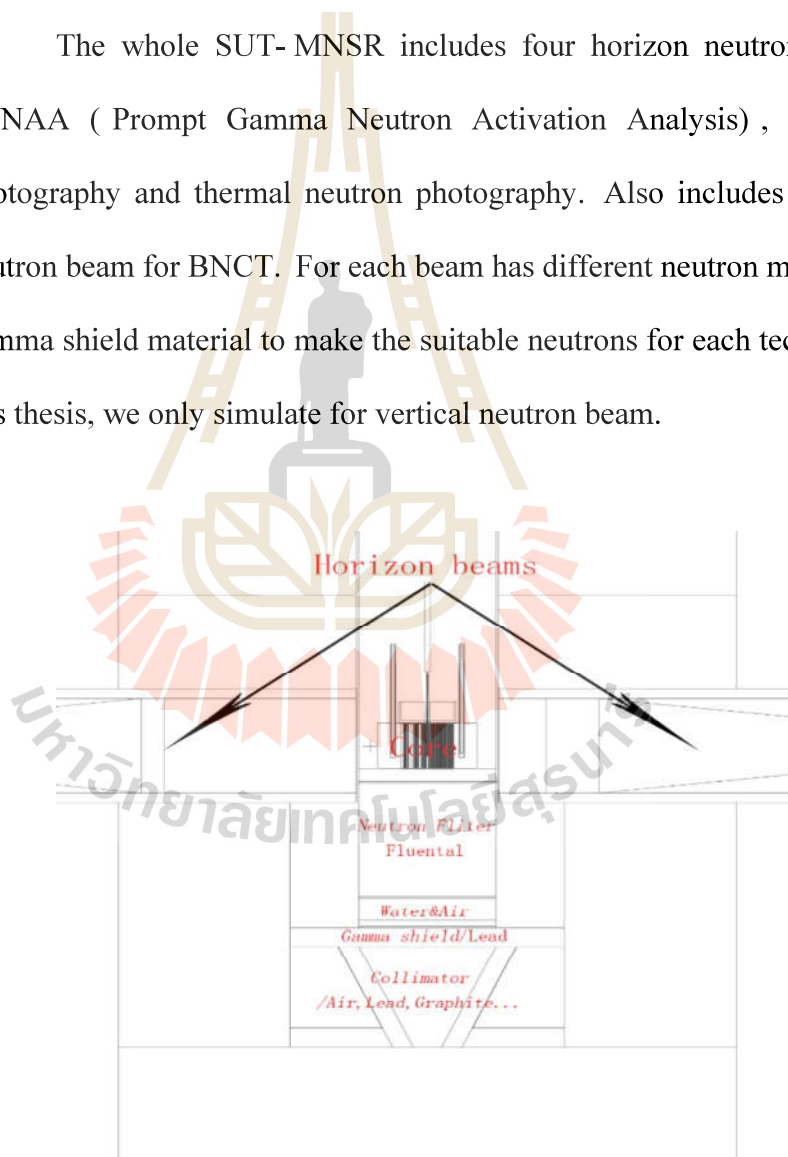
Figure 3.2 Fuel Assembly Diagram (MCNP).

Table 3.1 Grid position holes for SUT-MNSR element (CIAE).

Circle	1	2	3	4	5	6	7	8	9	10
Diameter /mm	21.9	43.8	65.7	87.6	109.5	131.4	153.3	175.2	197.1	219
Grid position hole	6	12	19	26	32	39	45	52	58	65

3.1.3 Whole Input Document

The whole SUT- MNSR includes four horizon neutron beams for PGNA (Prompt Gamma Neutron Activation Analysis) , fast neutron photography and thermal neutron photography. Also includes one vertical neutron beam for BNCT. For each beam has different neutron moderator and gamma shield material to make the suitable neutrons for each technology. In this thesis, we only simulate for vertical neutron beam.

**Figure 3.3** SUT-MNSR vertical neutron beam for BNCT (CIAE).

In Figure 3.3, neutrons will be produced at reactor core by fission reaction. During the neutrons (fast) pass through the neutron filter, the neutrons will be moderated to epi-thermal neutrons or thermal neutrons. Under neutron filter, we can shift the neutron spectrum by changing the thickness of water. Therefore, from one beam to get two kinds of neutron flux is proved to be successful. Figure 3.4 shows two kinds of neutron flux. Both of them are applied for BNCT for different kinds of cancer.

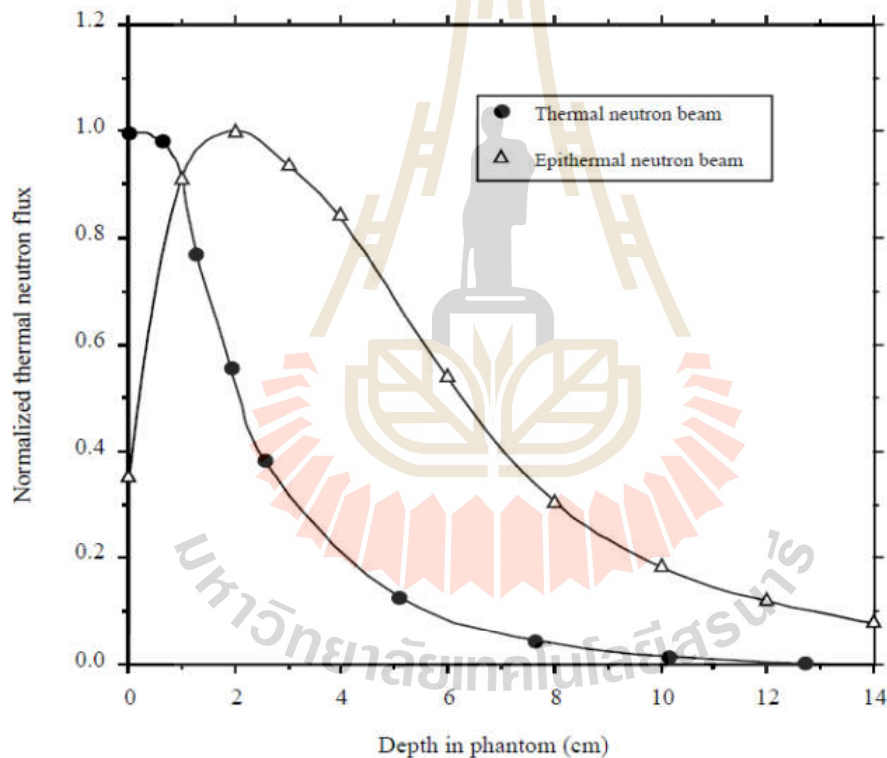


Figure 3.4 Changes of thermal neutron flux compared with epithermal neutron flux in phantom (Barth et al., 2005).

Following fuel assembly, neutron filter, water layer, gamma shield layer and collimator design and fuel elements are written as source card in MCNP. Finally, the whole MCNP input document for reactor structure

(surface card, cell card, material card and source card) was finished (Figure 3.5 and Figure 3.6).

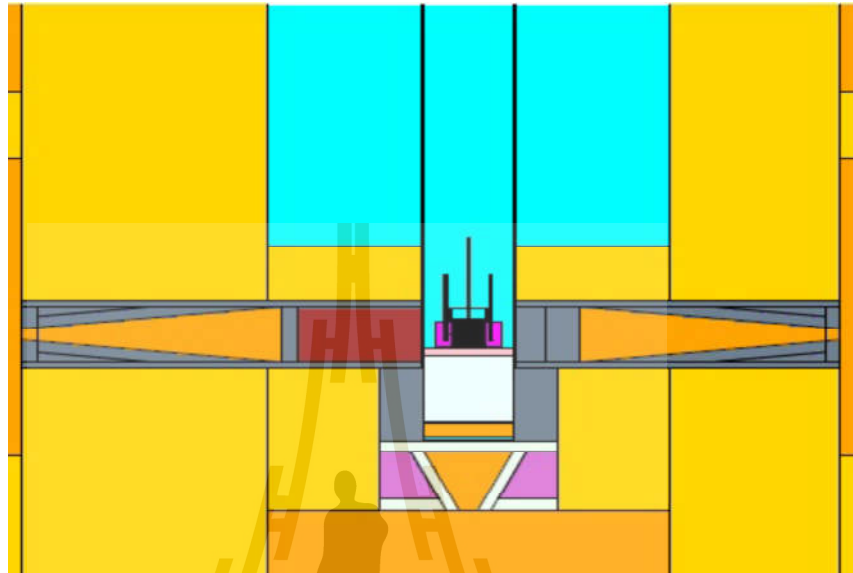


Figure 3.5 SUT-MNSR structure from MNCP (XZ basis).

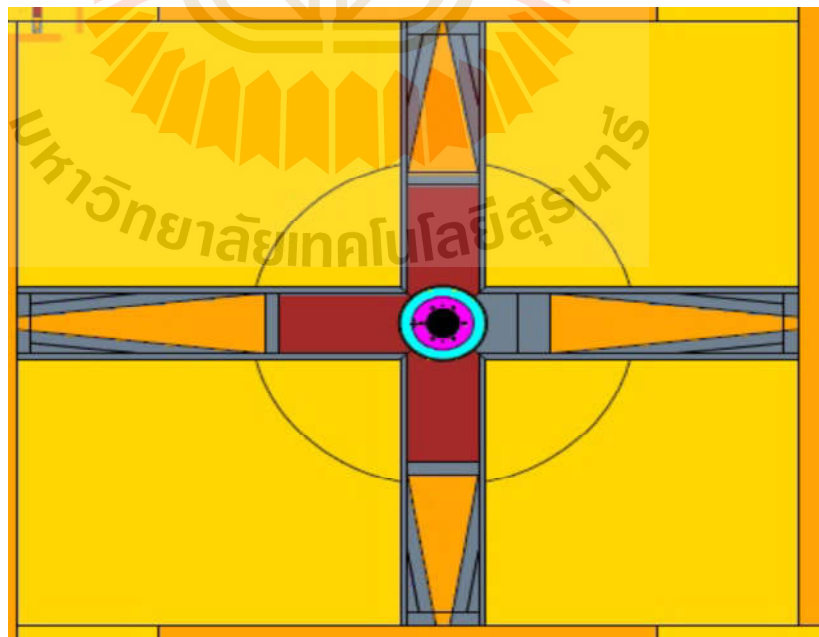


Figure 3.6 SUT-MNSR structure from MNCP (XY basis).

3.2 MCNP Input Document for Brain Model

Snyder brain model with three regions (ellipsoid) is selected as brain model. They are brain tissue, skull and the skin from the inner to outer of the model. This model has been used for BNCT neutron beam research by the Harvard-MIT group at MIT reactor for BNCT. The original Snyder brain only consists of two ellipsoids (cranium and brain). Then a 5mm thick has also been added as skin. Three parts boundary are shown in Equations 3.1 -3.3:

Between the air and scalp:

$$\left(\frac{x}{7.3}\right)^2 + \left(\frac{y}{10.3}\right)^2 + \left(\frac{z}{8.8}\right)^2 = 1 \quad (3.1)$$

Between the skull and scalp:

$$\left(\frac{x}{6.8}\right)^2 + \left(\frac{y}{9.8}\right)^2 + \left(\frac{z}{8.3}\right)^2 = 1 \quad (3.2)$$

Between the brain and skull:

$$\left(\frac{x}{6}\right)^2 + \left(\frac{y}{9}\right)^2 + \left(\frac{z}{6.5}\right)^2 = 1 \quad (3.3)$$

Figure 3.7 shows the section of the Snyder model.

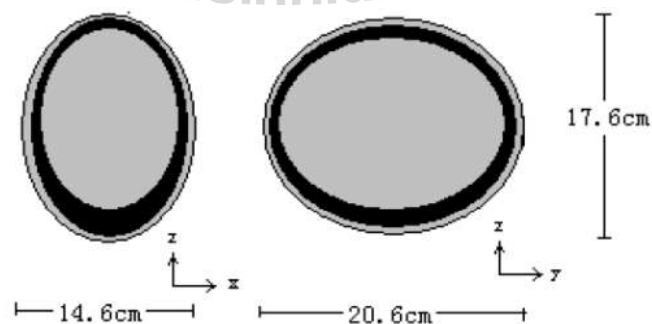


Figure 3.7 Cross section of Snyder model (Li et al., 2011).

The Snyder model can be written in MCNP surface card. The three regions will be three cells in MCNP input card. Then the material card for brain model can be written according to brain material of ICRU-46 report.

Z	element	Air	Skeleton-Cranium	Adult Whole brain	Adult skin
1	H	0	5.6	10.7	10
6	C	0.01	21.2	14.5	20.4
7	N	75.53	4	2.2	4.2
8	O	23.18	43.5	71.2	64.5
11	Na	0	0.1	0.2	0.2
12	Mg	0	0.2	0	0
15	P	0	8.1	0.4	0.1
16	S	0	0.3	0.2	0.2
20	Ca	1.28	17.6	0	0

Figure 3.8 Material densities and compositions in mass percent (Li et al., 2011).

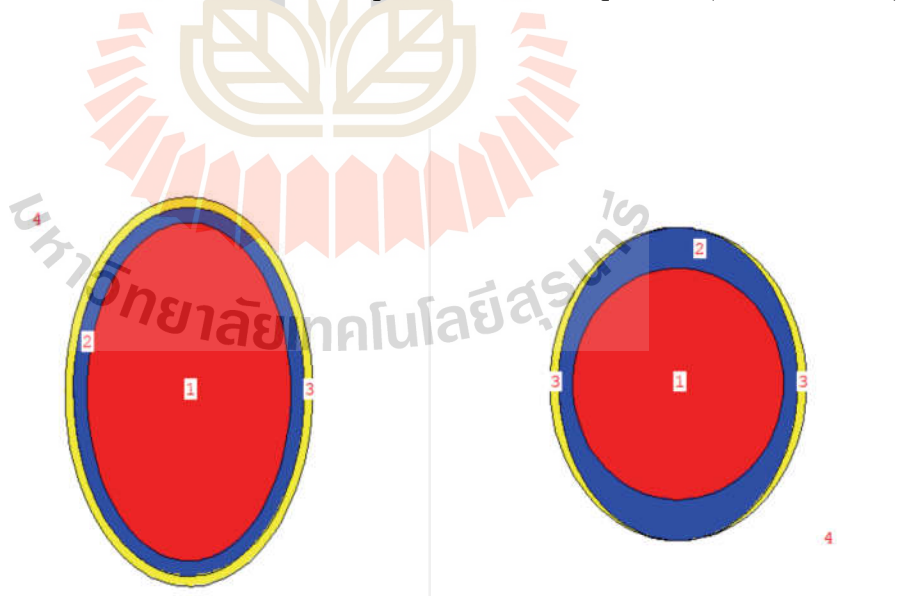


Figure 3.9 Snyder brain model from MCNP.

So finally we got the MCNP input document, reactor structure and Snyder brain model as shown in Figure 3.10.

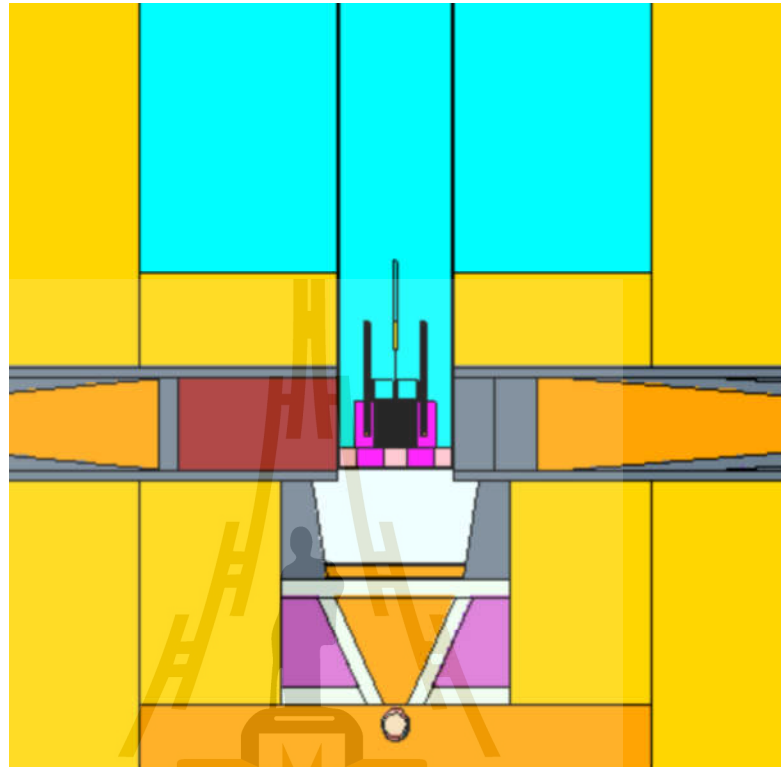


Figure 3.10 Reactor structure and Snyder brain model all in one from MCNP.

3.3 Tally method for Brain Model

The whole Snyder brain model neutron dose rate simulation, gamma dose rate simulation and energy deposition simulation (three dimensional) are finished by FMESH tally card. The FMESH card allows the user to define a mesh tally superimposed over the problem geometry. The output documents from simulation are written to the other one file (default name: MESHTAL MESHTAM) in units of particles/cm² or MeV/cm². Based on the FMESH tally method, the different DE and DF card to simulation for gamma, neutron dose rate and energy deposition are written. Figure 3.11 shows the FMESH tally method used for BNCT treatment planning.

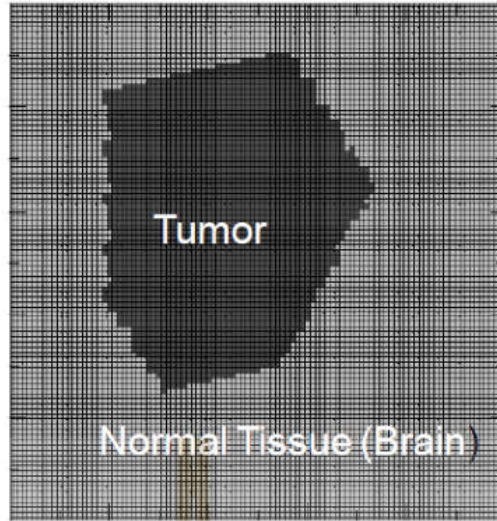


Figure 3.11 FMESH Mesh model (Kumada et al., 2011).

All of conversion factors are published by international organizations such as the National Council on Radiation Protection and Measurements (NCRP), the International Commission on Radiological Protection and Measurements (ICRP), the American National Standards Institute (ANSI) and the American Nuclear Society (ANS). The data changes based on the reevaluation of existing data and calculations or on the availability of new information. Currently, 1977 ANSI/ANS (Battat, 1977) conversion factors is underway and the ICRP and NCRP are considering an increase in the neutron quality factors by a factor of 2 to 2.5.

In summary, dose calculation:

$$dose = \int \Phi(E)Kerma(E)dE \quad (3.4)$$

And when a particle passes through the mesh j , the FMESH dose tally of the mesh is:

$$dose = \int \Phi(j,E)kerma(j,E) dE/V(j) \quad (3.5)$$

where $V(j)$ is the volume of the voxel.

3.3.1 Gamma Dose Rate Tally Card

MCNP presents gamma flux to dose rate conversion factor. It sets for use DE and DF tally cards to convert from calculated gamma flux to human biological dose equivalent rate. In this thesis gamma dose rate tally card tallied the result include both gamma dose come from reactor core (moderator) and brain tissue (hydrogen and nitrogen). Figure 3.12 shows gamma flux to dose rate conversion factor.

ANSI/ANS-6.1.1-1977		ICRP-21	
Energy, E (MeV)	DF(E) (rem/hr)/(p/cm ² -s)	Energy, E (MeV)	DF(E) (rem/hr)/(p/cm ² -s)
0.01	3.96E-06	0.01	2.78E-06
0.03	5.82E-07	0.015	1.11E-06
0.05	2.90E-07	0.02	5.88E-07
0.07	2.58E-07	0.03	2.56E-07
0.1	2.83E-07	0.04	1.56E-07
0.15	3.79E-07	0.05	1.20E-07
0.2	5.01E-07	0.06	1.11E-07
0.25	6.31E-07	0.08	1.20E-07
0.3	7.59E-07	0.1	1.47E-07
0.35	8.78E-07	0.15	2.38E-07
0.4	9.85E-07	0.2	3.45E-07
0.45	1.08E-06	0.3	5.56E-07
0.5	1.17E-06	0.4	7.69E-07
0.55	1.27E-06	0.5	9.09E-07
0.6	1.36E-06	0.6	1.14E-06
0.65	1.44E-06	0.8	1.47E-06
0.7	1.52E-06	1.	1.79E-06
0.8	1.68E-06	1.5	2.44E-06
1.0	1.98E-06	2.	3.03E-06
1.4	2.51E-06	3.	4.00E-06
1.8	2.99E-06	4.	4.76E-06
2.2	3.42E-06	5.	5.56E-06
2.6	3.82E-06	6.	6.25E-06
2.8	4.01E-06	8.	7.69E-06
3.25	4.41E-06	10.	9.09E-06
3.75	4.83E-06		
4.25	5.23E-06		
4.75	5.60E-06		
5.0	5.80E-06		
5.25	6.01E-06		
5.75	6.37E-06		
6.25	6.74E-06		

Figure 3.12 Photon Flux- to- Dose Rate Conversion Factors (Grande and O’Riordan, 1971).

3.3.2 Neutron Dose Rate Tally Card

Neutron dose rate tally card also come from neutron flux to dose conversion factor. So DE and DF card are different. The NCRP-38(Rossi, 1971) and ICRP-21 (Grande, 1971) quality factor and neutron flux to dose conversion factor are listed in Figure 3.13. In this thesis, neutron dose rate comes from SUT-MNSR BNCT beam line.

Energy, E (MeV)	DF(E) (rem/hr)/(n/cm ² -s)	Quality Factor	DF(E) (rem/hr)/(n/cm ² -s)	Quality Factor
2.5E-08	3.67E-06	2.0	3.85E-06	2.3
1.0E-07	3.67E-06	2.0	4.17E-06	2.0
1.0E-06	4.46E-06	2.0	4.55E-06	2.0
1.0E-05	4.54E-06	2.0	4.35E-06	2.0
1.0E-04	4.18E-06	2.0	4.17E-06	2.0
1.0E-03	3.76E-06	2.0	3.70E-06	2.0
1.0E-02	3.56E-06	2.5	3.57E-06	2.0
1.0E-01	2.17E-05	7.5	2.08E-05	7.4
5.0E-01	9.26E-05	11.0	7.14E-05	11.0
1.0	1.32E-04	11.0	1.18E-04	10.6
2.0			1.43E-04	9.3
2.5	1.25E-04	9.0		
5.0	1.56E-04	8.0	1.47E-04	7.8
7.0	1.47E-04	7.0		
10.0	1.47E-04	6.5	1.47E-04	6.8
14.0	2.08E-04	7.5		
20.0	2.27E-04	8.0	1.54E-04	6.0

Figure 3.13 Neutron Flux-to-Dose Rate Conversion Factors.

3.3.3 Energy Deposition Tally Card

The F6 energy deposition tally card in units of MeV/g and *F6 changes the units to jerks/g ($1\text{MeV} = 1.6021910^{-22}\text{ jerks}$). MCNP computes energy deposition with a heating function [H (E) or Q] modifying a track length reaction rate tally (Equation 3.6). In other words, the average energy deposited

for all reactions at the incident particle energy is used in the tally. For BNCT, energy deposition tally card is applied to calculate the physical absorbed doses. In BNCT theory, most boron neutron capture reaction will happen at tumor area because of a high boron concentrate rate. And the reactions produce high linear energy transfer particle. In other word, the energy deposition at tumor area should be more than normal tissue area. This guess will be corroborated in next chapter (energy deposition result).

$$H(E) = E - \sum_i p_i(E) [\overline{E_{i,out}}(E) - Q_i + \overline{E_{i,\gamma}}(E)] \quad (3.6)$$

where $p_i = \frac{\sigma_i(E)}{\sigma_T(E)}$ = probability of reaction i at neutron incident energy E ,

$\overline{E_{i,out}}(E)$ = average exiting neutron energy for reaction i at neutron incident energy E ,

$\overline{E_{i,\gamma}}(E)$ = average exiting gamma energy for reaction i at neutron incident energy E ,

Q_i = Q-value of reaction i

CHAPTER IV

RESULT AND DISSCUSSION

Based on the simulation methods mentioned in the previous chapter, we simulated two Snyder brain model. One is normal brain model named “Brain model”. The other one is Snyder brain model carrying 40 ppm boron at tumor area (guess) and 10 ppm boron at normal tissue area named “B-containing brain model”. We simulated for two models because “B-containing brain model” can be used for the calculation of the energy deposition contribution from boron neutron reaction part. This is a primary physical absorb dose for BNCT. The “Brain model” only can be used for the calculation of energy deposition in normal tissue.

In addition, SUT-MNSR BNCT beam with two kinds of neutron flux is proved to be successful (previous chapter). But it is difficult to calculate brain model for all of neutron energy spectrum. The changing of neutron energy spectrum by the thickness of water is shown in Figure 4.1. So we choose neutron energy spectrum at thickness of water equal to 0 cm. From SUT-MNSR (30 kW) simulation result (MCNP), we choose thickness of water equal to 0 cm, the epi-thermal neutron flux is much higher than IAEA suggestion ($1 \times 10^9 n cm^2 s^{-1}$). Moreover the fast neutron contamination and thermal neutron contamination is only $6.9 \times 10^7 n cm^2 s^{-1}$ and $7.3 \times 10^7 n cm^2 s^{-1}$, respectively. Altogether, SUT-MNSR BNCT beam shows a reasonable incident beam quality for BNCT.

All of MCNP simulation results are in unit of dose rate/ source neutron or energy deposition/ source neutron. We can multiply source neutron by the SUT-MNSR reactor power as shown in equation:

$$\left(\frac{1 \text{ joule/sec}}{\text{watt}}\right) \left(\frac{1 \text{ MeV}}{1.602 \times 10^{-13} \text{ joules}}\right) \left(\frac{\text{fission}}{180 \text{ MeV}}\right) = 3.467 \times 10^{10} \frac{\text{fissions}}{\text{watt}} / \text{sec} \quad (4.1)$$

Therefore, to produce P watts of power, one needs $3.467 \times 10^{10} P$ fissions per second. This power level produces $3.467 \times 10^{10} \times P \times \bar{\nu}$, which is the neutron source strength per second for power P in watts. For an average $\bar{\nu}$ of 2.6 neutrons/fission, the neutron source strength is $9.0 \times 10^{10} P$ neutrons/sec. So we can estimate that SUT-MNSR source strength is $\approx 2.7 \times 10^{15}$ neutrons/sec.

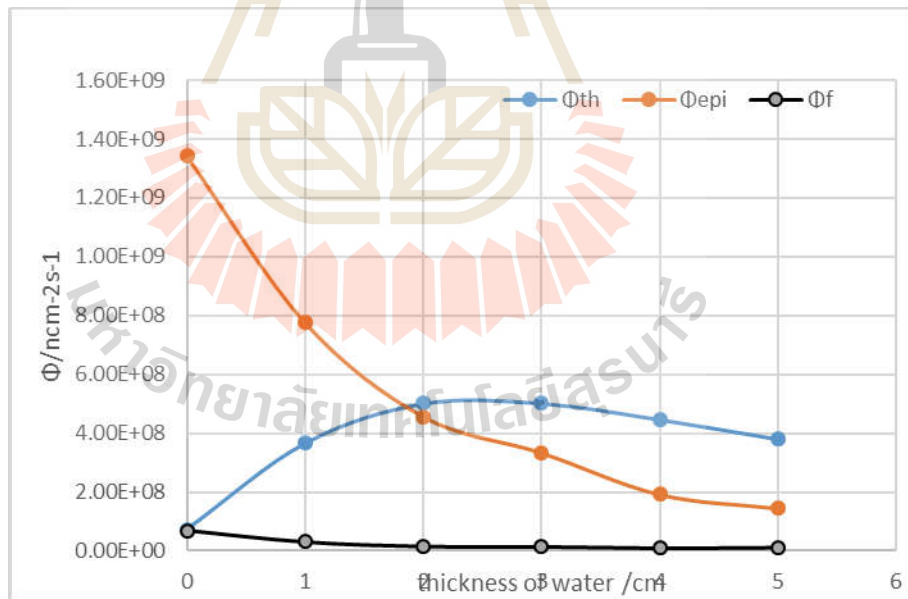


Figure 4.1 Changing of neutron energy spectrum by thickness of water (MCNP).

4.1 Gamma Dose Rate

The gamma dose rate is primary from reactor core contamination and hydrogen and nitrogen neutron capture gamma reaction. Also will come from boron neutron capture reaction (0.477MeV) or other reaction but can be ignored. First we got gamma dose rate result from F5 :p tally card at BNCT outlet of $7.2822 \times 10^{-14} \text{Gy cm}^2 \text{n}^{-1}$. IAEA suggests value at outlet of facility of $\leq 13 \times 10^{-13} \text{Gy cm}^2 \text{n}^{-1}$. But gamma dose rate should be increased after neutron beam enter brain model because of hydrogen and nitrogen neutron capture gamma reaction contribution (hydrogen and nitrogen come from brain, skin, skull tissue. See figure 3.7). Figure 4.2-4.5 show the gamma dose rate result in brain model.

Figure 4.5 shows the increasing of gamma dose rate after neutron beam enter brain model based on MCNP FMESH tally card simulation result.

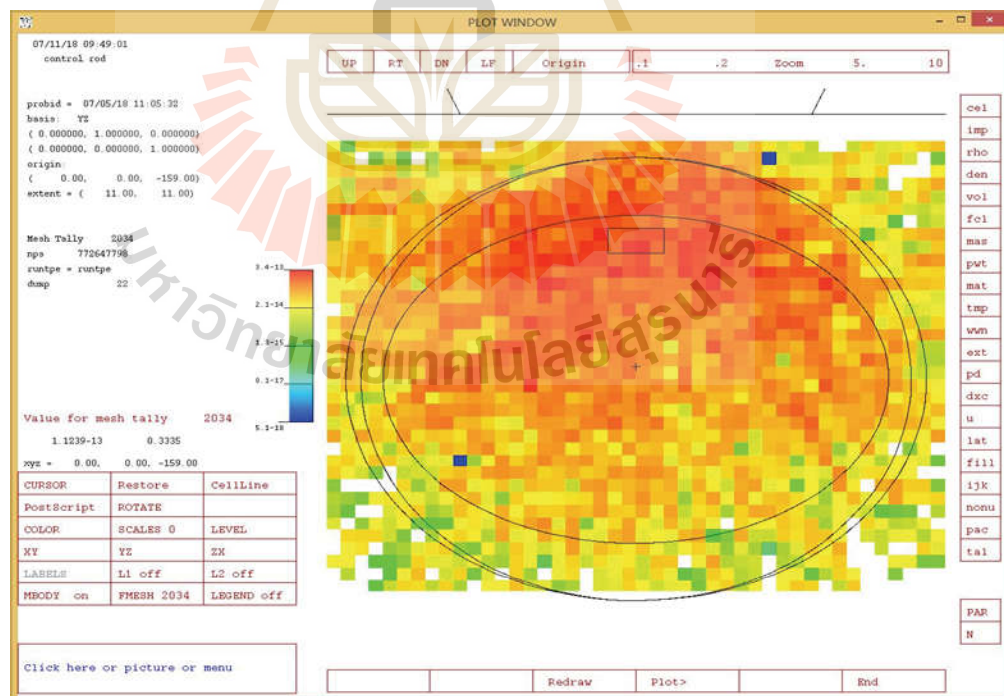


Figure 4.2 Gamma dose rate YZ basis (MCNP).

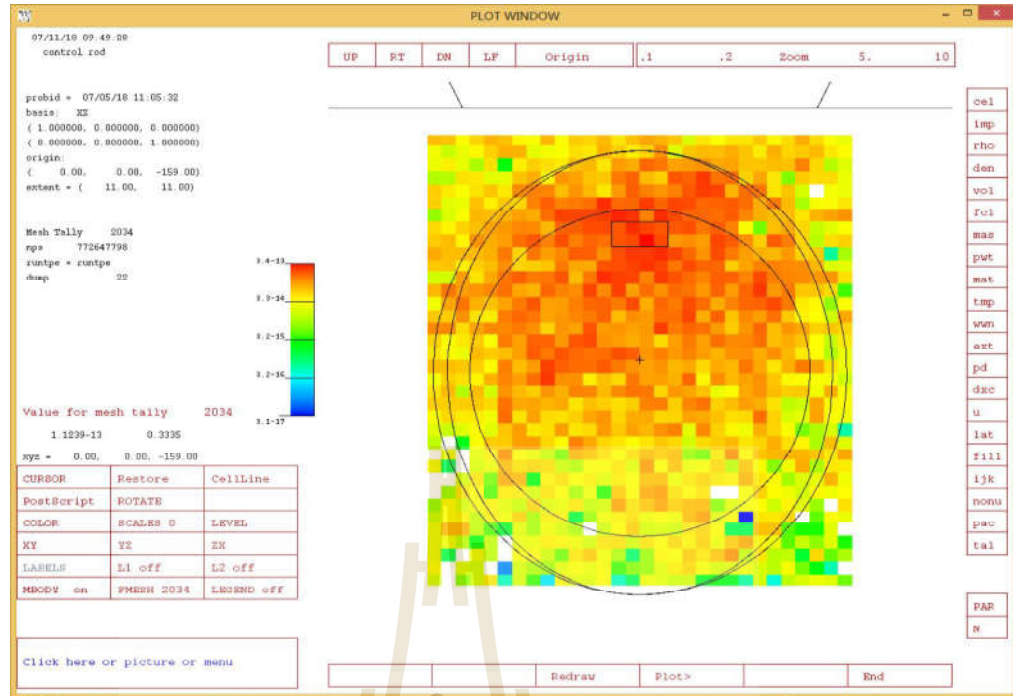


Figure 4.3 Gamma dose rate XZ basis (MCNP).

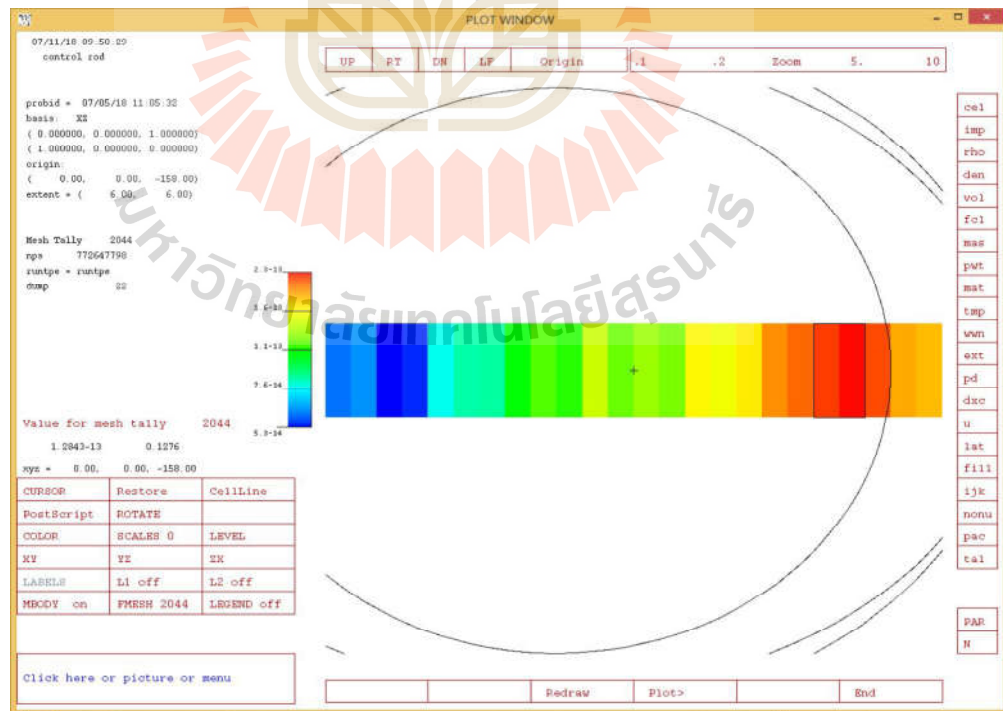


Figure 4.4 Changing of gamma dose rate by depth of brain model (MCNP).

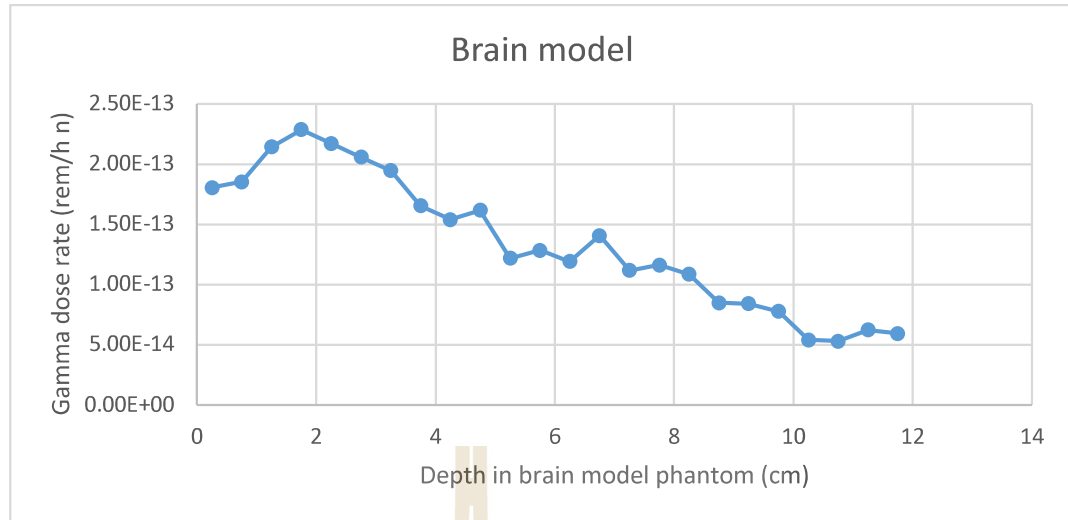


Figure 4.5 Changing of gamma dose rate by depth of brain model.

4.2 Neutron Dose Rate

For the neutron dose rate, we got two simulation results. There are Brain model neutron dose result and B-containing brain model result. Both of them are simulated using the same FMESH tally method. Finally, we got the neutron dose rate result in units of 0.01Gy/h n. The tumor area for B-containing brain model is a small cylinder in the center with 2 cm depth. The brain model neutron dose rate result is the same as B-containing brain result (Figure 4.10), because both of them are simulated from same neutron source and same MCNP dose tally card based on flux tally card and conversion factor.

The DE card is used to simulation “thermal” neutron dose rate, “epi-thermal” neutron dose rate and fast neutron dose rate.

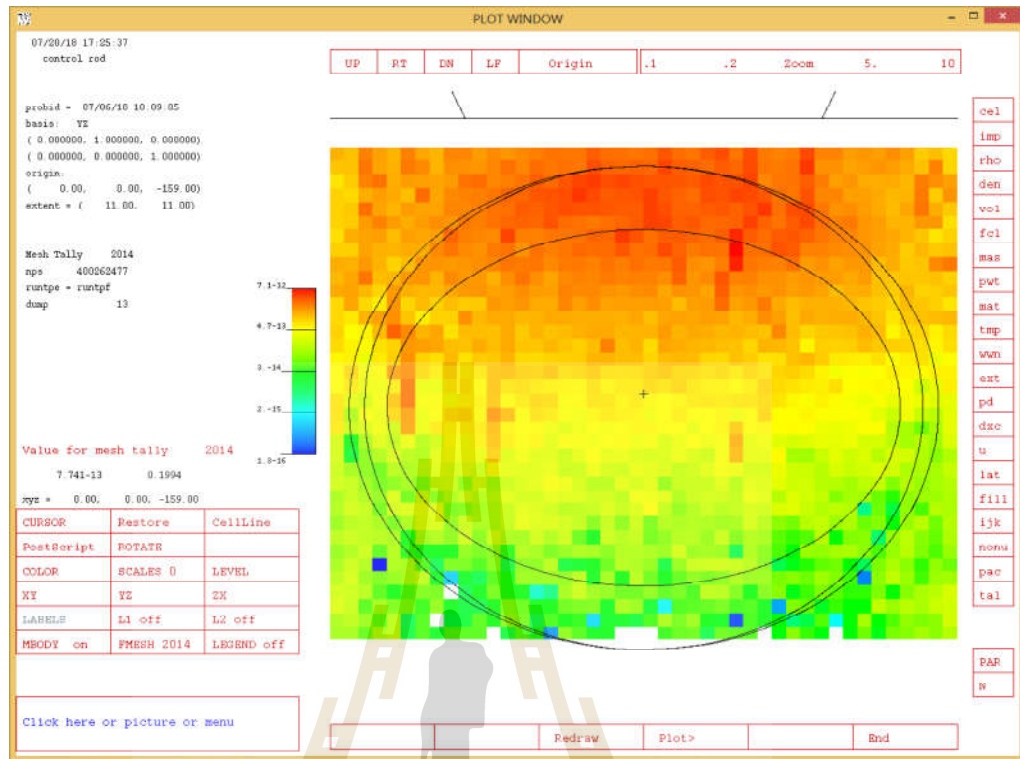


Figure 4.6 Neutron dose rate for brain model YZ basis (MCNP).

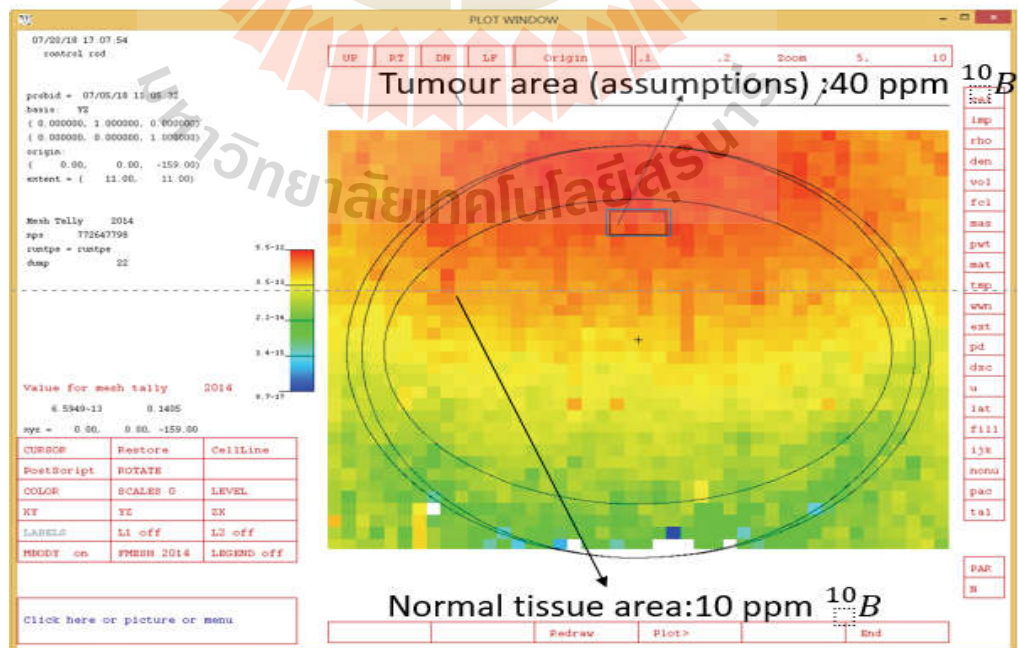


Figure 4.7 Neutron dose rate for B-containing brain model YZ basis (MCNP).

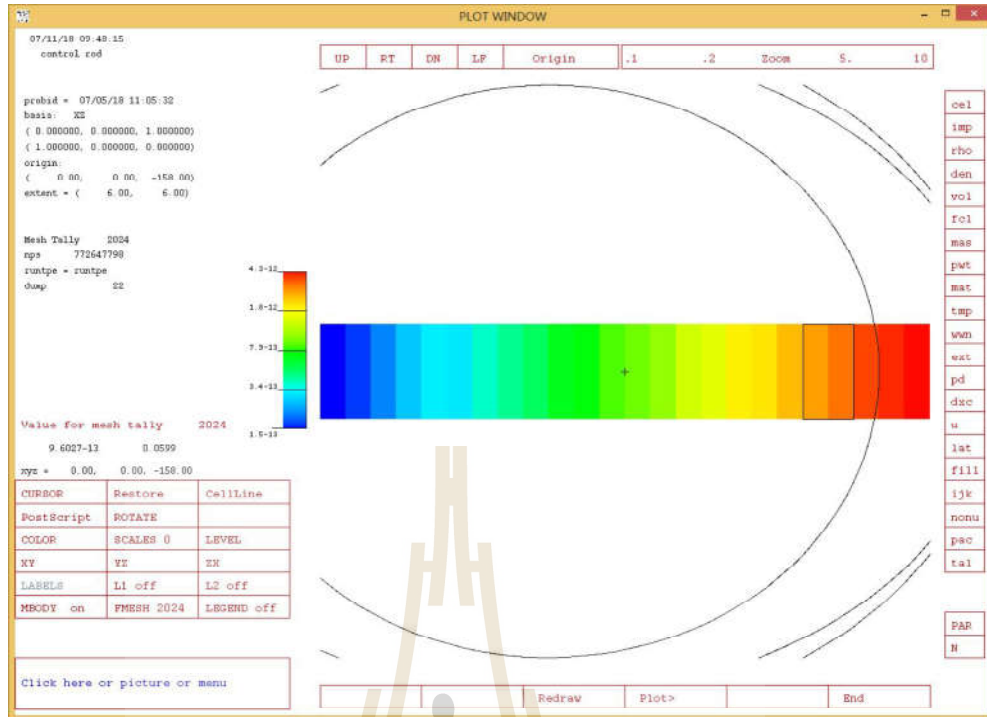


Figure 4.8 Changing of neutron dose rate for B-containing brain model by depth (MCNP).

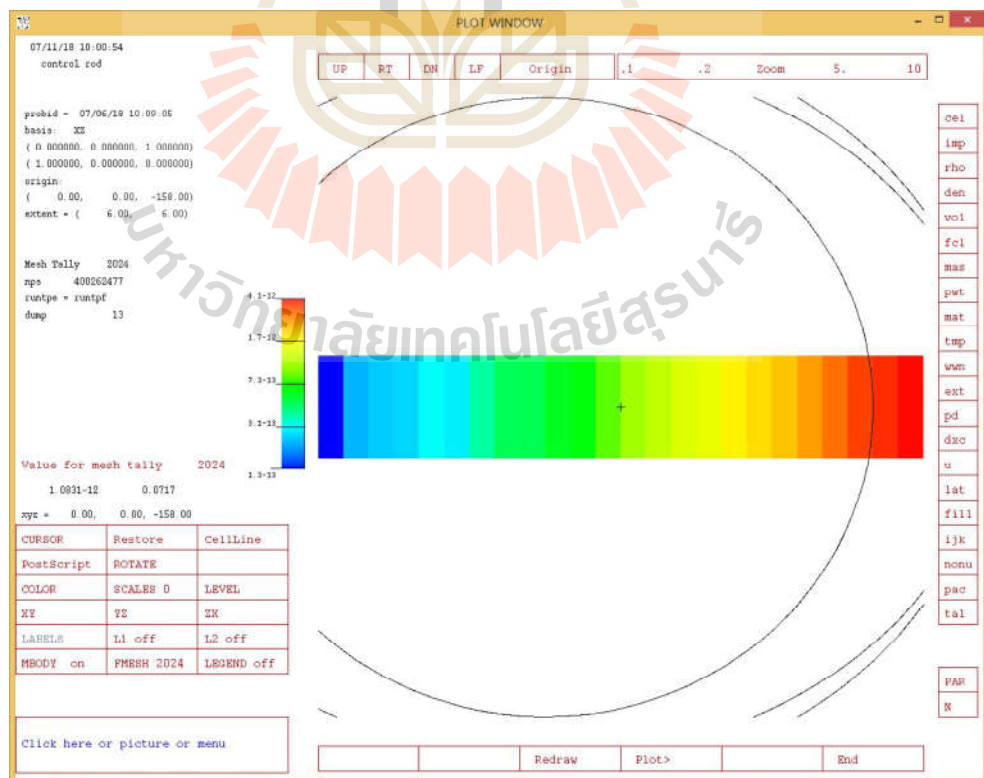


Figure 4.9 Changing of neutron dose rate for brain model by depth (MCNP).

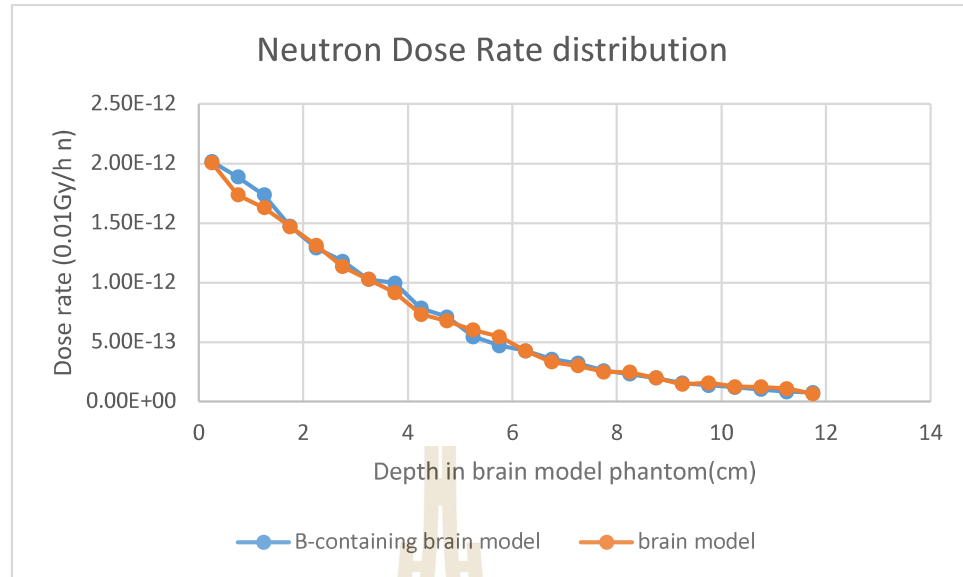


Figure 4.10 Changing of neutron dose rate for brain model by depth.

4.3 Energy Deposition

In the energy deposition result, it is obvious that the value of energy deposition for B-containing brain model at tumor area is much higher than the brain model at the same area. At normal area, the value of energy deposition for B-containing brain model is higher than brain model at the same area. The reason is that the thermal neutron boron capture reactions occur on tumor area. This result can be used to prove that SUT-MNSR will be successful for BNCT.

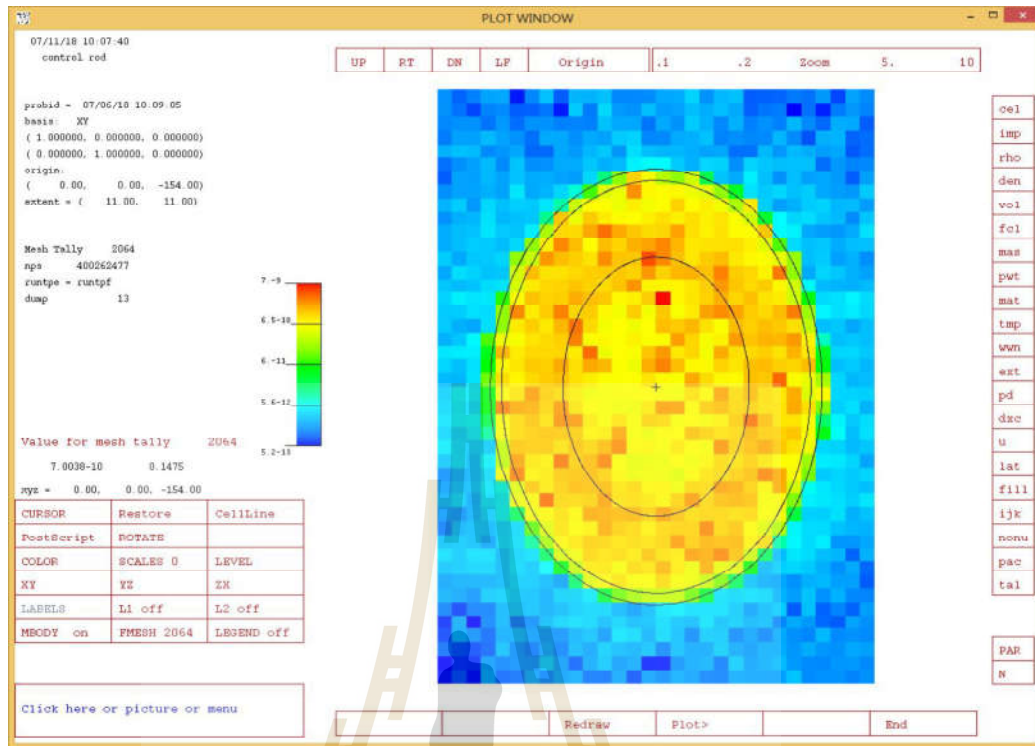


Figure 4.11 Energy deposition for brain model (MCNP).

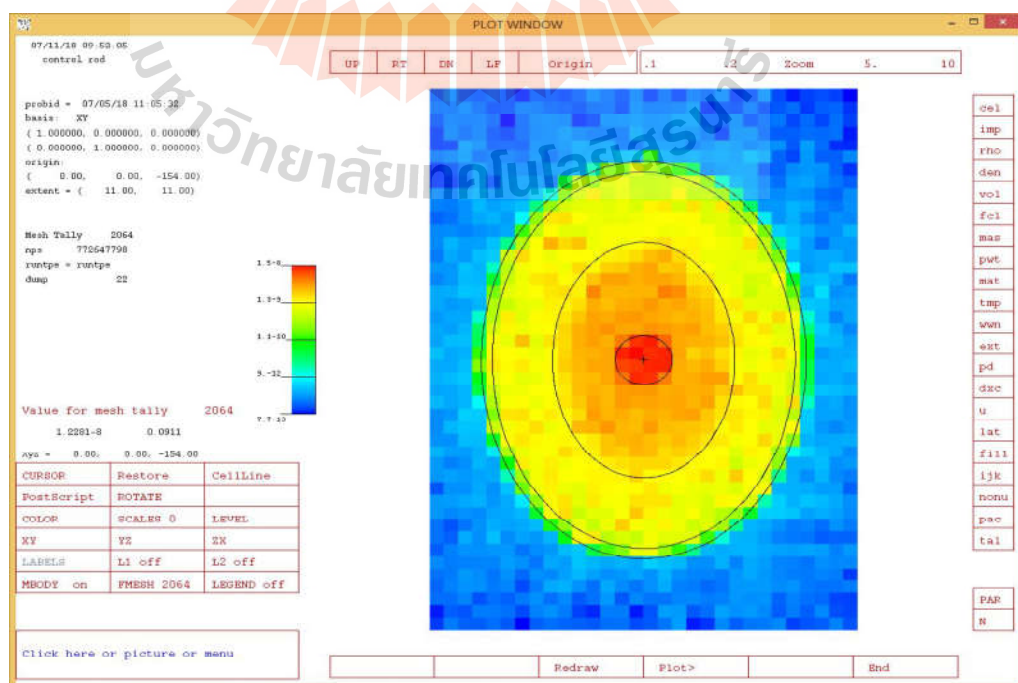


Figure 4.12 Energy deposition for B-containing brain model (MCNP).

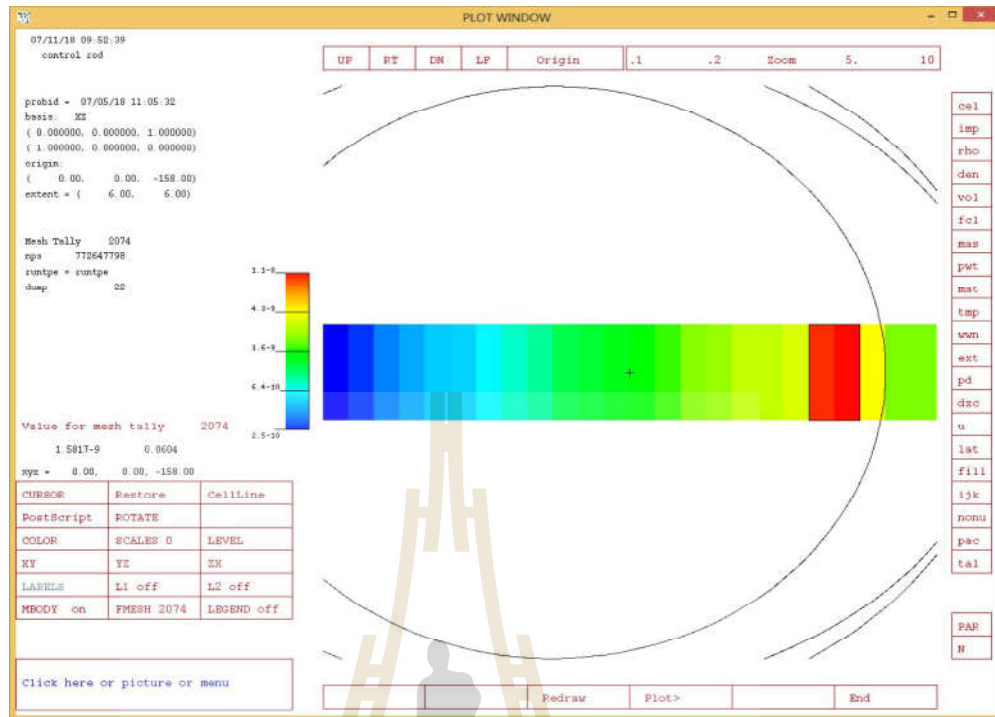


Figure 4.13 Changing of energy deposition for B-containing brain model by depth (MCNP).

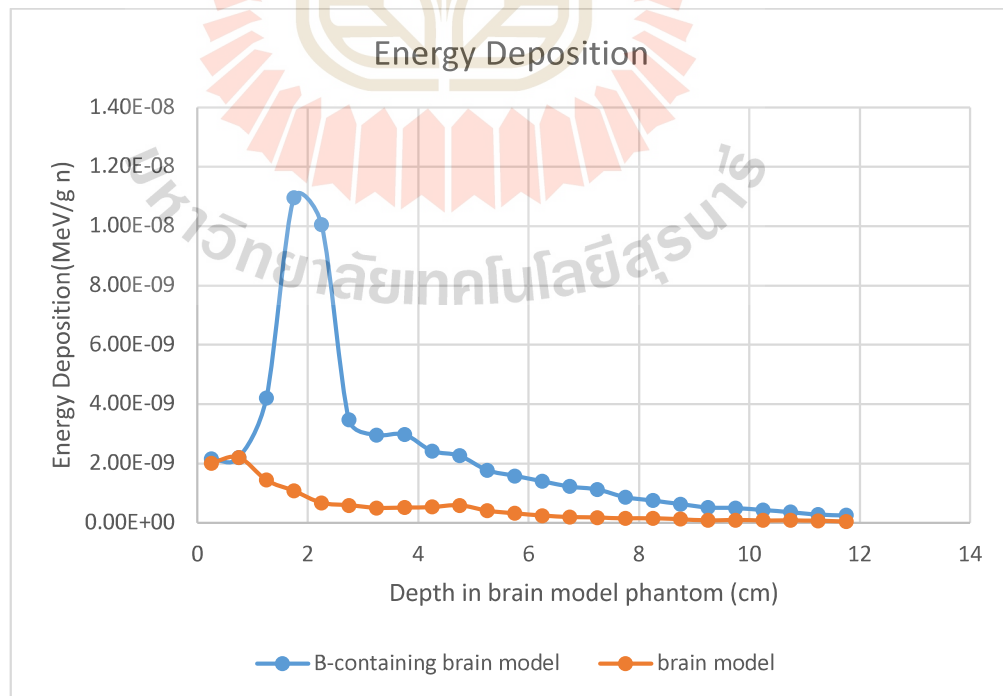


Figure 4.14 Changing of energy deposition by depth.

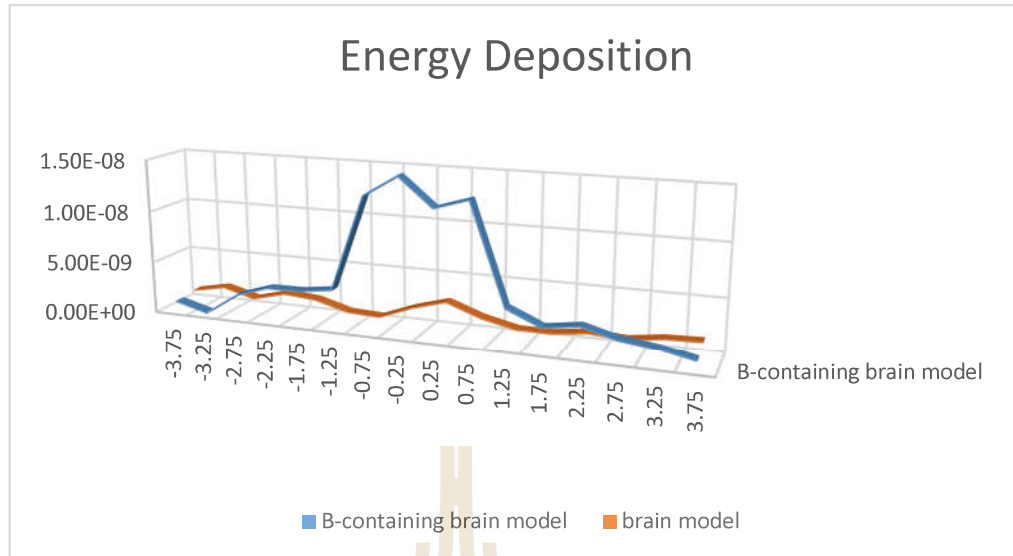


Figure 4.15 Energy deposition horizontal cross-section (depth in brain model 2cm).

4.4 Discussion and Conclusion

In this thesis the two types of brain models, brain model and B-containing brain model, are studied. The simulations are performed four times for each model. We enhanced the “nps” from 17003270 (first time) to 400262477 (last time). The last time simulation has been optimized for reducing the relative errors. For the first time simulation, each model consists of $15 \times 22 \times 18 = 5940$ cubes (Figure 4.16) in FMESH tally card. But for the last time, each model consists of $30 \times 44 \times 36 = 47520$ cubes (Figure 4.17). Figure 4.17 shows clear boundary for each cubes. FMESH tally can be used to calculate the average dose rate in each smaller cube. On the other hand, the last time MCNP simulation takes a long time about 19 hours for each model (computer: Intel(R) Xeon(R) CPU E5-2680 v3 @2.50 Hz).

Moreover, the BNCT can be used for liver cancer and breast cancer treatment, the dose rate simulation is required and should be studied in the near future.

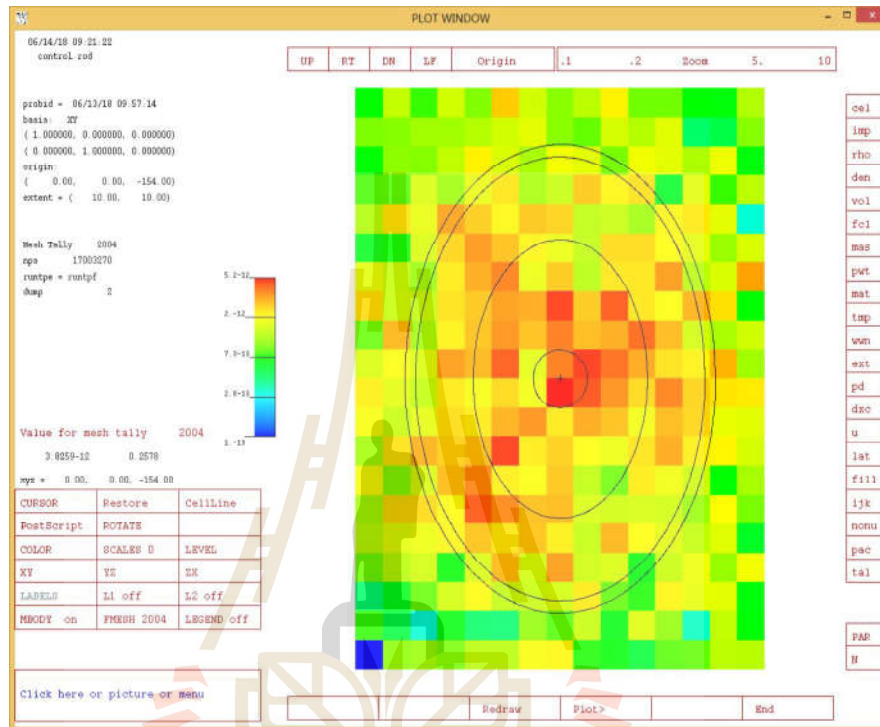


Figure 4.16 15*22*18=5940 cubes model.

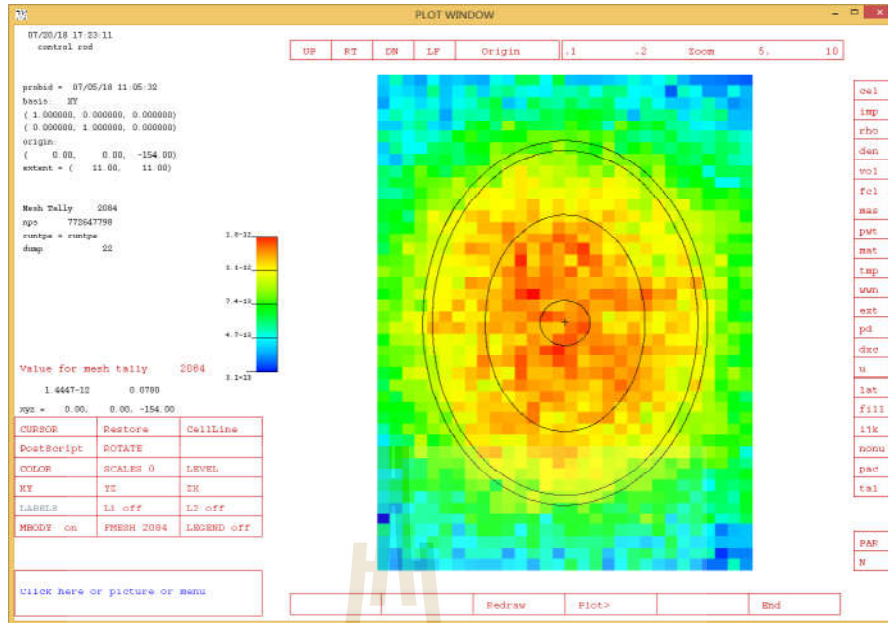
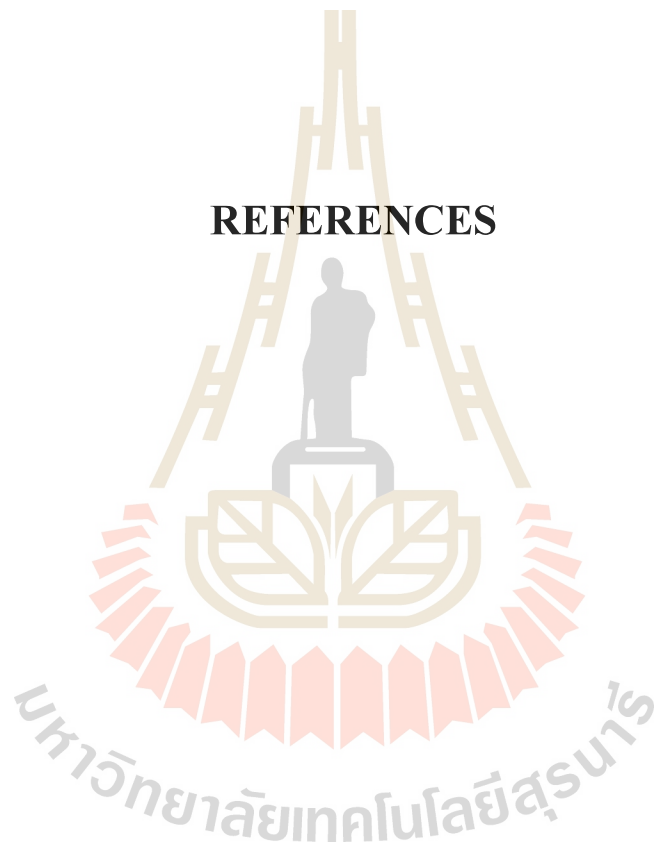


Figure 4.17 $30 \times 44 \times 46 = 47520$ cubes model.

REFERENCES



REFERENCES

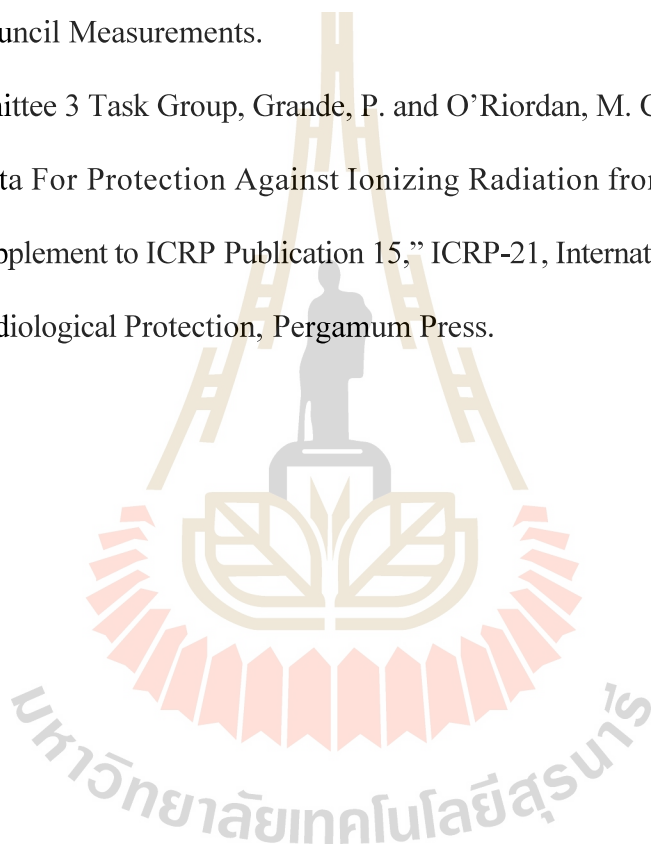
- Taylor, H. J., and Goldhaber, M. (1935). Detection of nuclear disintegration in a photographic emulsion. **Nature (London)**. 135: 341-348
- Locher, G. L. (1936). Biological effects and therapeutic possibilities of neutrons. **Am J Roentgenol Radium Ther.** 36(1): 1-13
- Sweet, W. H., and Javid, M. (1951). The possible use of slow neutrons plus boron-10 in the therapy of intracranial tumors. **Trans Am Neurol Assoc.** 76: 60-63
- Archambeau, J. O. (1970). The effect of increasing exposures of the $^{10}\text{B} (n,\alpha) ^7\text{Li}$ reaction on the skin of man. **Radiology.** 94: 178-187
- Hatanaka, T. (1969). Future possibility of neutron capture therapy of malignant tumors by use of low energy neutron from nuclear reactors and other sources. **Gan No Rinsho.** 15(4): 367-369
- X-5 Monte Carlo Team. (2003). MCNP- A General Monte Carlo N-Particle Transport Code Version 5.
- Barth, R. F., Coderre, J. A., Vicente, M. G. H., and Blue, T. E. (2005). Boron neutron capture therapy of cancer: current status and future prospects. **Clinical Cancer Research.** 11(11): 3987-4002
- Yoshinobu, N. (2006). Boron Neutron Capture Therapy in Japan. **ICNCT-12.** 1:7 - 638
- Glasstone, S., and Milton C. Edlund. (1958). Nuclear Reactor Theory. **State Scientific Publishing House.** 56: 2-3

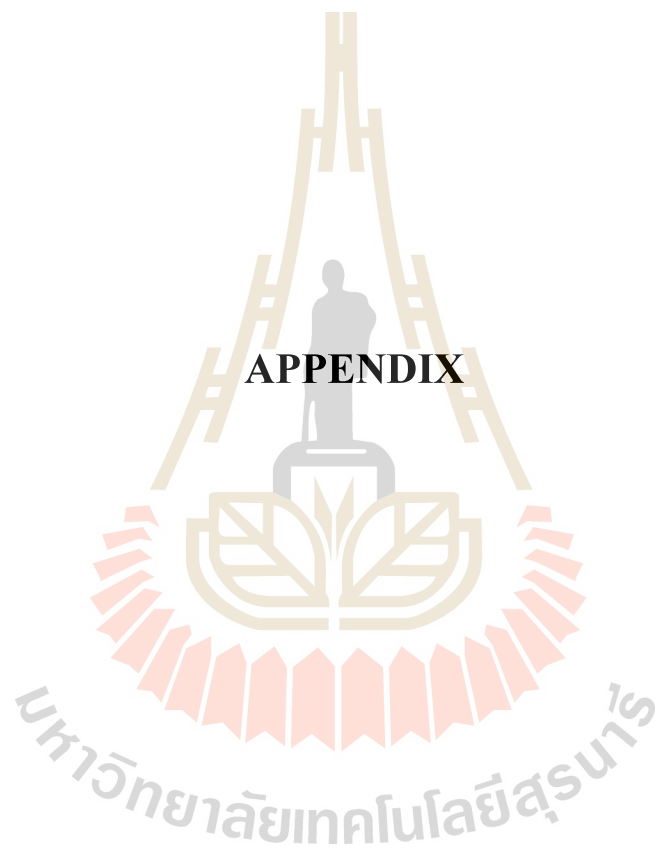
- David, W. N., Floyd, J. W., Daniel, E. W., Jacek, C., and Manjeet, C. (1997). Computational dosimetry and treatment planning for boron neutron capture therapy. **J Neurooncol.** 33(1-2): 93-104.
- Briesmeister, J F., MCNP (1997). A General Monte Carlo N Particle Transport Code. LA12625- M, Version 4B ed., Los **Alamos: Los Alamos National Laboratory.**
- Paul, M. B., Otto, K. H., Matthew, R. P., KigerIII, W S., Jody, K., Irving, K., Cynthia, F. C., Tim, G. J., Kent J. R., Thomas, H. N., Gustavo, A., Santa C., Xing-Qi, L., and Robert, G. Z. (2003). Critical Examination of the Results from the Harvard-MIT NCT Program Phase I Clinical Trial of Neutron Capture Therapy for Intracranial Disease. **Journal of Neuro-Oncology.** 62: 111-121
- Kumada¹, H., Yamamoto¹, K., Matsumura, A., Yamamoto, T., and Nakagawa, Y. (2007). Development of JCDS, a computational dosimetry system at JAEA for boron neutron capture therapy. **J. Phys.: Conf. Ser.** 74: 021010
- Li, D., Chaobin, C., Tao, Y., and Gang, L. (2011). The Dosimetry Calculation for Boron Neutron Capture Therapy. InTech DOI: 10.5772/22270.
- ICRP Committee 3 Task Group, Grande, P., O’Riordan, M. C., and Chairmen (2019). Data for Protection Against Ionizing Radiation from External Sources: Supplement to CRP Publication 15, ICRP-21, International Commission on Radiological Protection Pergamon Press (April 19) 71
- Kumadaa, H., Saitob, K., Nakamurab, T., Sakaea, T., Sakuraia, H., Matsumurac, A., and Ono, K. (2011). Multistep Lattice-Voxel method utilizing lattice function for Monte-Carlo treatment planning with pixel based voxel model. **Applied Radiation and Isotopes** Volume 69 Issue 12

ANS-6.1.1 Working Group and Battat, M. E. (Chairman) (1977). American National Standard Neutron and Gamma-Ray Flux-to-Dose Rate Factors ANSI/ANS-6.1.1-1977 (N666)

American Nuclear Society, LaGrange Park, Illinois. NCRP Scientific Committee 4 on Heavy Particles and Rossi, H. H. (Chairman) (1971). Protection Against Neutron Radiation NCRP-38, on Radiation Protection and National Council Measurements.

ICRP Committee 3 Task Group, Grande, P. and O’Riordan, M. C. (Chairmen) (1971). Data For Protection Against Ionizing Radiation from External Sources: Supplement to ICRP Publication 15,” ICRP-21, International Commission on Radiological Protection, Pergamum Press.





APPENDIX

1. MCNP FMESH card used in this thesis

FMESH2014:N GEOM=XYZ ORIGIN=-7.5 -11 -168 \$ 不同能量中子剂量三维分布

rem/h

IMESH=7.5 IINTS=30

JMESH=11 JINTS=44

KMESH=-150 KINTS=36

OUT=IJ

DE2014 2.50E-08 1.00E-07 5.00E-07 1.00E-06 1.00E-05 1.00E-04 1.00E-03

1.00E-02 1.00E-01 5.00E-01 1.0 2.5 5.0 7.0 10.0 14.0 20.0

DF2014 3.67E-06 3.67E-06 3.67E-06 4.46E-06 4.54E-06 4.18E-06 3.76E-06 &

3.56E-06 2.17E-06 9.26E-05 1.32E-04 1.25E-04 1.56E-04 1.47E-04 &

1.47E-04 2.08E-04 2.27E-04

FMESH2024:N GEOM=XYZ ORIGIN=-1 -1 -164 \$ 不同能量中子剂量轴向分布

rem/h

IMESH=1 IINTS=1

JMESH=1 JINTS=1

KMESH=-152 KINTS=24

OUT=JK

DE2024 2.50E-08 1.00E-07 5.00E-07 1.00E-06 1.00E-05 1.00E-04 1.00E-03

1.00E-02 1.00E-01 5.00E-01 1.0 2.5 5.0 7.0 10.0 14.0 20.0

DF2024 3.67E-06 3.67E-06 3.67E-06 4.46E-06 4.54E-06 4.18E-06 3.76E-06 &
 3.56E-06 2.17E-06 9.26E-05 1.32E-04 1.25E-04 1.56E-04 1.47E-04 &
 1.47E-04 2.08E-04 2.27E-04

FMESH2034:P GEOM=XYZ ORIGIN=-7.5 -11 -168 \$伽马剂量三维分布 rem/h

IMESH=7.5 IINTS=30

JMESH=11 JINTS=44

KMESH=-150 KINTS=36

OUT=IJ

DE2034 0.01 0.03 0.05 0.07 0.1 0.15 0.2 0.25 0.3 0.35 0.4 0.45 0.5 0.55 &
 0.6 0.65 0.7 0.8 1 1.4 1.8 2.2 2.6 2.8 3.25 3.75 4.25 4.75 5 5.25 &
 5.75 6.25 6.75 7.5 9 11 13 15

DF2034 3.96E-06 5.82E-07 2.90E-07 2.58E-07 2.83E-07 3.79E-07 5.01E-07 &
 6.31E-07 7.59E-07 8.78E-07 9.85E-07 1.08E-06 1.17E-06 1.27E-06 &
 1.36E-06 1.44E-06 1.52E-06 1.68E-06 1.98E-06 2.51E-06 2.99E-06 &
 3.42E-06 3.82E-06 4.01E-06 4.41E-06 4.83E-06 5.23E-06 5.60E-06 &
 5.80E-06 6.01E-06 6.37E-06 6.74E-06 7.11E-06 7.66E-06 8.77E-06 &
 1.03E-05 1.18E-05 1.33E-05

FMESH2044:P GEOM=XYZ ORIGIN=-1 -1 -164 \$伽马剂量轴向分布 rem/h

IMESH=1 IINTS=1

JMESH=1 JINTS=1

KMESH=-152 KINTS=24

OUT=JK

DE2044 0.01 0.03 0.05 0.07 0.1 0.15 0.2 0.25 0.3 0.35 0.4 0.45 0.5 0.55 &
 0.6 0.65 0.7 0.8 1 1.4 1.8 2.2 2.6 2.8 3.25 3.75 4.25 4.75 5 5.25 &

5.75 6.25 6.75 7.5 9 11 13 15

DF2044 3.96E-06 5.82E-07 2.90E-07 2.58E-07 2.83E-07 3.79E-07 5.01E-07 &
 6.31E-07 7.59E-07 8.78E-07 9.85E-07 1.08E-06 1.17E-06 1.27E-06 &
 1.36E-06 1.44E-06 1.52E-06 1.68E-06 1.98E-06 2.51E-06 2.99E-06 &
 3.42E-06 3.82E-06 4.01E-06 4.41E-06 4.83E-06 5.23E-06 5.60E-06 &
 5.80E-06 6.01E-06 6.37E-06 6.74E-06 7.11E-06 7.66E-06 8.77E-06 &
 1.03E-05 1.18E-05 1.33E-05

c FMESH2054:N GEOM=XYZ ORIGIN=-7.5 -11 -168 \$F7

c IMESH=7.5 IINTS=30

c JMESH=11 JINTS=44

c KMESH=-150 KINTS=36

c OUT=IJ

c FM2054 -1 0 -6 -8

FMESH2064:N GEOM=XYZ ORIGIN=-7.5 -11 -168 \$F6

IMESH=7.5 IINTS=30

JMESH=11 JINTS=44

KMESH=-150 KINTS=36

OUT=IJ

FM2064 -1 0 1 -4

FMESH2074:N GEOM=XYZ ORIGIN=-1 -1 -164 \$不同能量轴向中子能量沉积

IMESH=1 IINTS=1

JMESH=1 JINTS=1

KMESH=-152 KINTS=24

OUT=JK

FM2074 -1 0 1 -4

FMESH2084:N GEOM=XYZ ORIGIN=-7.5 -11 -168 \$中子剂量三维分布 gy/100

IMESH=7.5 IINTS=30

JMESH=11 JINTS=44

KMESH=-150 KINTS=36

OUT=IJ

DE2084 2.50E-08 1.00E-07 1.00E-06 1.00E-05 1.00E-04

1.00E-03 1.00E-02 1.00E-01 5.00E-01 1 2.5 5 7 10 14 20

DF2084 1.84E-06 1.84E-06 2.23E-06 2.27E-06 2.09E-06

1.88E-06 1.42E-06 2.89E-06 8.42E-06 1.20E-05

1.39E-05 1.95E-05 2.10E-05 2.26E-05 2.77E-05 2.84E-05

FMESH2094:N GEOM=XYZ ORIGIN=-1 -1 -164 \$中子剂量轴向分布 gy/100

IMESH=1 IINTS=1

JMESH=1 JINTS=1

KMESH=-152 KINTS=24

OUT=JK

DE2094 2.50E-08 1.00E-07 1.00E-06 1.00E-05 1.00E-04

1.00E-03 1.00E-02 1.00E-01 5.00E-01 1 2.5 5 7 10 14 20

DF2094 1.84E-06 1.84E-06 2.23E-06 2.27E-06 2.09E-06

1.88E-06 1.42E-06 2.89E-06 8.42E-06 1.20E-05

1.39E-05 1.95E-05 2.10E-05 2.26E-05 2.77E-05 2.84E-05

2. MCNP M card used in this thesis

c -----19.75%U-5 enrichment UO₂ fuel pellets density=10.6

m1 8016.60C -0.118482929 \$ O
 92235.60C -0.114362057 \$ U-235
 92238.60C -0.76138734 \$ U-238
 92232.60C -4.39854E-08 \$ U-232
 92234.60C -0.001759416 \$ U-234
 92236.60C -0.00219927 \$ U-236
 43099.60C -4.39854E-06 \$ Tc -99
 13027.60C -0.000219927 \$ Al
 6000.60C -8.79708E-05 \$ C
 20000.60C -8.79708E-05 \$ Ca
 12000.60C -8.79708E-05 \$ Mg
 17000.60C -2.19927E-05 \$ Cl
 24000.50c -0.000219927 \$ Cr
 27059.60C -8.79708E-05 \$ Co
 9019.60C -1.31956E-05 \$ F
 1001.60C -1.14362E-06 \$ H
 26000.55c -0.000439854 \$ Fe
 28000.50C -2.19927E-05 \$ Ni
 7014.60C -6.59781E-05 \$ N
 14000.60C -0.000439854 \$ Si
 90232.60C -8.79708E-06 \$ Th-232

c -----Zr density=6.5

m2 40000.60c -0.9783105 \$ Zr

50000.42c	-0.017	\$ Sn
26000.55c	-0.0024	\$ Fe
28000.50c	-7E-05	\$ Ni
24000.50c	-0.0013	\$ Cr
13027.60c	-7.5E-05	\$ Al
5010.60c	-9.15555E-08	\$ B-10
5011.66c	-4.084445E-07	\$ B-11
48000.50c	-5E-07	\$ Cd
27059.60c	-2E-05	\$ Co
29000.50c	-5E-05	\$ Cu
72000.60c	-0.0001	\$ Hf
12000.60c	-2E-05	\$ mg
25055.60c	-5E-05	\$ mn
42000.60c	-5E-05	\$ mo
82000.50c	-0.00013	\$ pb
14000.60c	-0.00012	\$ si
22000.60c	-5E-05	\$ ti
92238.60c	-3.5E-06	\$ U-238
23000.60c	-5E-05	\$ V
74000.55c	-0.0001	\$ w
17000.60c	-0.0001	\$ cl

c -----

c ---s.s ---0Cr18Ni11Ti density=7.9

m3 24000.50c -0.18 \$ Cr

25055.60c -0.02 \$ mn

26000.55c -0.6744 \$ fe
 28000.50c -0.11 \$ ni
 22000.60c -0.006 \$ ti
 14000.60c -0.008 \$ si
 6000.60c -0.0006 \$ c
 27059.60c -0.0003 \$ co
 15031.60c -0.0004 \$ p
 16000.60c -0.0003 \$ s
 c -----
 c ---He ----density=1.6094e-4
 m4 2004.60c -1
 c -----
 c ----water density=0.9982-----
 m5 1001.60c -1.12E-01 \$ h
 8016.60c -8.88E-01 \$ o
 17000.60c -6.00E-08 \$ cl
 29000.50c -5.00E-08 \$ cu
 26000.55c -5.00E-08 \$ fe
 mt5 lwtr.01t
 c -----
 c ----Be density=1.82
 m6 4009.60c -0.99734796581 \$ be
 26000.55c -0.00175 \$ fe
 13027.60c -0.00034 \$ al

14000.60c	-7.5E-05	\$ si
12000.60c	-7E-05	\$ mg
28000.50c	-9.2E-05	\$ ni
24000.50c	-5.6E-05	\$ cr
25055.60c	-2E-05	\$ mn
8016.60c	-1.04E-06	\$ o
30000.42c	-1E-05	\$ zn
29000.50c	-0.00012	\$ cu
27059.60c	-4E-06	\$ co
47000.55c	-1.2E-06	\$ ag
5010.60c	-2.2109E-07	\$ b-10
5011.66c	-9.7891E-07	\$ b-11
3006.60c	-6.2383E-08	\$ li-6
3007.60c	-8.97617E-07	\$ li-7
48000.50c	-4E-07	\$ cd
7014.60c	-0.00011	\$ n
62149.50c	-3.419E-08	\$ sm-149
63000.35c	-1E-07	\$ Eu
64000.35c	-1E-07	\$ gd

mt6 be.01t

c -----

c ----air ---density=0.001293

m7 8016.60c -3.08E-01 \$ o

7014.60c -6.92E-01 \$ n

c -----

c ----- LT21 Al density=2.7

m8 13027.60c -9.8150E-01 \$ al

26000.55c -2.0000E-03 \$ fe

14000.60c -9.8000E-03 \$ si

28000.50c -3.0000E-04 \$ ni

29000.50c -1.0000E-04 \$ cu

25055.60c -1.0000E-04 \$ mn

22000.60c -1.0000E-04 \$ ti

12000.60c -5.8000E-03 \$ mg

30000.42c -3.0000E-04 \$ zn

3006.60c -1.2996E-07 \$ li-6

3007.60c -1.8700E-06 \$ li-7

5010.60c -1.8424E-07 \$ b-10

5011.66c -8.1576E-07 \$ b-11

48000.50c -1.0000E-06 \$ cd

c -----

c -----Cd --- density=8.64

m9 48000.50c -1 \$ Cd

c -----

c -----graphite density=1.686

m10 6000.60c -0.99998724 \$ C

5010.60c -2.5794E-09 \$ B-10

5011.66c -1.14206E-08 \$ b-11

17000.60c	-2.9E-06	\$ cl
25055.60c	-2E-08	\$ mn
12000.60c	-6.38E-07	\$ mg
14000.60c	-4.8E-06	\$ si
26000.55c	-1.85E-06	\$ fe
28000.50c	-3E-07	\$ ni
13027.60c	-1.218E-06	\$ al
20000.60c	-8.2E-07	\$ ca
22000.60c	-1E-07	\$ ti
23000.60c	-1E-07	\$ v
MT10 grph.01t		
c -----		
c -----	Pb density=11.35	
m11 82000.50c	-9.999796E-01	\$ pb
47000.55c	-1.700000E-06	\$ ag
29000.50c	-1.200000E-06	\$ cu
51000.42c	-1.200000E-06	\$ sb
33075.35c	-1.000000E-06	\$ as
83209.60c	-1.059000E-05	\$ bi
50000.42c	-1.010000E-06	\$ sn
30000.42c	-1.000000E-06	\$ zn
26000.55c	-2.700000E-06	\$ fe

c -----

c -----

c -----fluent density=2.85

m12 13027.60c -5.218E-1 \$ al

3006.60C -2.023E-4 \$ li-6

3007.60c -2.473E-3 \$ li-7

9019.60c -4.755E-1 \$ f

c -----

c ----- Al₂O₃ density=3.965

m13 13027.60c -0.52941176471 \$ al

8016.60c -0.47058823529 \$ o

c -----

c ----concrete density=3.45

m14 13027.60c -0.026800088159 \$ al

1001.60c -0.081996539005 \$ h

8016.60c -0.51247836878 \$ o

26000.55c -0.23290759042 \$ fe

14000.60c -0.03264072054 \$ si

25055.60c -0.00032562762947 \$ mn

16000.60c -0.00014440716078 \$ s

15031.60c -0.014924548125 \$ p

22000.60c -0.0004300413075 \$ ti

24000.50c -0.0071722223187 \$ cr

12000.60c -0.044636290519 \$ mg

20000.60C -0.044636290519 \$ ca

23000.60c -0.00090726552023 \$ v

c -----

c -BeF2 density=1.9860

m15 4009.60c 1 9019.60c 2

c -----

c -B4C density=2.508-2.512

m16 5010.60c 19.8 5011.66c 80.2 6000.60c 25

c -----

c -B4C density=2.508-2.512

m17 5011.60c 4 6000.60c 1

c -----

c ----concrete density=3.45

m18 13027.60c -0.026800088159 \$ al

1001.60c -0.081996539005 \$ h

8016.60c -0.51247836878 \$ o

26000.55c -0.23290759042 \$ fe

14000.60c -0.03264072054 \$ si

25055.60c -0.00032562762947 \$ mn

16000.60c -0.00014440716078 \$ s

15031.60c -0.014924548125 \$ p

22000.60c -0.0004300413075 \$ ti

24000.50c -0.0071722223187 \$ cr

12000.60c -0.044636290519 \$ mg

20000.60C -0.044636290519 \$ ca

23000.60c -0.00090726552023 \$ v

c -----

c ----Bi density=9.8

m19 83209.60c -0.999981 \$ bi

33075.35c -5E-06 \$ as

29000.50c -2E-06 \$ cu

47000.55c -1E-06 \$ ag

30000.42c -1E-06 \$ zn

82000.50c -1E-06 \$ pb

51000.42c -1E-06 \$ sb

17000.60c -3E-06 \$ cl

26000.55c -5E-06 \$ fe

c -----

c -----

c 无水氟化铝 density=3.0

m20 9019.60c -6.553E-01

13027.60c -3.384E-01

11023.60c -3.223E-03

14000.60c -5.013E-04

8016.60c -1.664E-03

26000.55c -4.512E-04

16000.60c -3.581E-04

15031.60c -1.407E-04

c -----

c ----B-poly density=0.9804618 10%碳化硼

m21 6000.60c -0.79341557 \$ -0.79341557

1001.60c -0.12857143 \$ -0.12857143

5010.60c -0.01409955 \$ -0.01409955

5011.66c -0.06290045 \$ -0.06290045

9019.60c -2.5E-06 \$ -2.5E-06

17000.60c -7.5E-06 \$ -7.5E-06

20000.60c -3E-06 \$ -3E-06

26000.55c -0.001 \$ -0.001

c -----

c ----- Pb-B-poly -----

M22 1001.60c -0.0271429

6000.60c -0.1658206

5010.60c -0.001433045

5011.66c -0.006393055

82000.50C -0.7992

29000.50c -3.2E-6

50000.42c -4e-6

30000.42c -3.2e-6 \$ density=-3.6

c --- LiF -poly density=

m23 6000.60c -0.25714285714 \$ c

1001.60c -0.042857142857 \$ h

3006.60c -0.014160609729 \$ li-6

3007.60c -0.17314904277 \$ li-7

9019.60c -0.5126903475 \$ F

c -----新材料-----

m25 13027.60c 5.2179E-01

9019.60c 4.7554E-01

3006.60c 1.7358E-04

3007.60c 2.4976E-03

c -----

c -----新材料-----

m26 13027.60c 4.5393E-01

9019.60c 5.4340E-01

3006.60c 1.7358E-04

3007.60c 2.4976E-03

c -----

c -----新材料-----

m27 13027.60c 4.2000E-01

9019.60c 5.7733E-01

3006.60c 1.7358E-04

3007.60c 2.4976E-03

c -----

c -----新材料-----

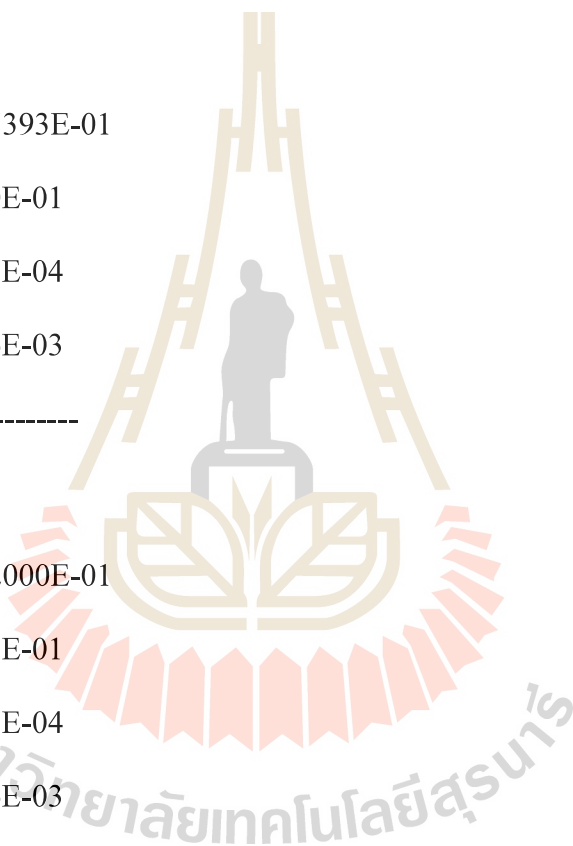
m28 13027.60c 3.8607E-01

9019.60c 6.1126E-01

3006.60c 1.7358E-04

3007.60c 2.4976E-03

c -----



c -----新材料-----

m29 13027.60c 3.1821E-01

9019.60c 6.7911E-01

3006.60c 1.7358E-04

3007.60c 2.4976E-03

c -----

c ----heavy water density=1.106-----

m99 1002.60c 0.667 \$ D

8016.60c 0.333 \$ o

c -----brain tissue icru-----

m87 1001.60C -0.107 \$H

6000.60C -0.145 \$C

7014.60C -0.022 \$N

8016.60C -0.712 \$O

11023.60C -0.002 \$NA

15031.60C -0.004 \$P

16000.60C -0.002 \$S

17000.60C -0.003 \$CL

19000.60C -0.003 \$K

c -----skull-----

m88 1001.60C -0.056 \$H

6000.60C -0.212 \$C

7014.60C -0.04 \$N

8016.60C -0.435 \$O

11023.60C -0.001 \$NA

12000.60C -0.002 \$MG

15031.60C -0.081 \$P

16000.60C -0.003 \$\$

20000.60C -0.176 \$Ca

c -----skin-----

c m89 1001.60C -0.1 \$H

c 60000.60C -0.204 \$C

c 70147.60C -0.042 \$N

c 8016.60C -0.645 \$O

c 11023.60C -0.002 \$Na

c 16000.60C -0.001 \$\$

c 17000.60c -0.003 \$Cl

c 19000.60c -0.001 \$K

c -----skin-----

m89 1001.60C -0.1 \$H

6000.60C -0.204 \$C

7014.60C -0.042 \$N

8016.60C -0.645 \$O

11023.60C -0.002 \$Na

16000.60C -0.001 \$\$

17000.60c -0.003 \$Cl

19000.60c -0.001 \$K

CURRICULUM VITAE

NAME: Kaijian Li

GENDER: Male

NATIONALITY: Chinese

DATE OF BIRTH: May 9, 1992

EDUCATIONS:

M.Sc. Department of Nuclear Science and Technology, University of South of China, China, 2011.

PUBLICATIONS

F. Liu, Y. Q. Shi, K. J. Li, "Measurement of Effective Delayed Neutron Fraction for ADS Venus 1# Sub-criticality Reactor 50(8), Atomic energy science and technology, 1445-1448.

